Spatial and temporal distribution of cell wall polysaccharides during grain development of Brachypodium distachyon

Mathilde Francin-Allami, Camille Alvarado, Sylviane Daniel, Audrey Geairon, Luc Saulnier, Fabienne Guillon

Spatial and temporal distribution of cell wall polysaccharides during grain development of *Brachypodium distachyon*.

Mathilde Francin-Allami, Camille Alvarado, Sylviane Daniel, Audrey Geairon, Luc Saulnier, Fabienne Guillon

INRA, UR 1268 Biopolymères Interactions Assemblages, 44000 Nantes, France

Corresponding author: Dr Mathilde Francin-Allami, INRA, UR 1268 Biopolymères Interactions Assemblages, 44000 Nantes, France

E-mail: mathilde.francin-allami@inra.fr

Fax: +33(0) 2 40 67 50 84

Plant Science

Abstract

Brachypodium distachyon (Brachypodium) is now well considered as being a suitable plant model for studying temperate cereal crops. Its cell walls are phylogenetically intermediate between rice and poaceae, with a greater proximity to these latter. By microscopic and biochemical approaches, this work gives an overview of the temporal and spatial distribution of cell wall polysaccharides in the grain of Brachypodium from the end of the cellularization step to the maturation of grain. Variation in arabinoxylan chemical structure and distribution were demonstrated according to development and different grain tissues. In particular, the kinetic of arabinoxylan feruloylation was shown occuring later in the aleurone layers compared to storage endosperm. Mixed linked β-glucan was detected in whole the tissues of Brachypodium grain even at late stage of development. Cellulose was found in both the storage endosperm and the outer layers. Homogalacturonan and rhamnogalacturonan I epitopes were differentially distributed within the grain tissues. LM5 galactan epitope was restricted to the aleurone layers contrary to LM6 arabinan epitope which was detected in the whole endosperm. A massive deposition of highly methylated homogalacturonans in vesicular bodies was observed underneath the cell wall of the testa t2 layer at early stage of development. At maturity, low-methylated homogalacturonans totally fulfilled the lumen of the t2 cell layer, suggesting pectin remodeling during grain development. Xyloglucans were only detected in the cuticle above the testa early in the development of the grain while feruloylated arabinoxylans were preferentially deposited into the cell wall of t1 layer. Indeed, the circumscribed distribution of some of the cell wall polysaccharides raises questions about their role in grain development and physiology.

Keywords : *Brachypodium distachyon* ; Grain development ; Cell wall ; Polysaccharides

Highlights :

- Distribution of polysaccharides during *B. distachyon* grain development.
- Fine structure of arabinoxylans varies according to tissue and grain development.
- Amazing distribution of polysaccharides highlighted into the testa of *B. distachyon* grain.

60 **Abbreviations**

61 MLG : mixed linked β-glucan

62 AX : Arabinoxylan

63 HG: Homogalacturonan

64 RGI : Rhamnogalacturonan I

65 DAF : day after flowering

66

67

68

69

70

71

72

73

74

75

76

77

78

79

80

81

1. Introduction

For several years *Brachypodium distachyon* (Brachypodium) is considered as a model plant for temperate grasses such as wheat and barley because of its phylogenetic proximity to the cereal crops, but also for its small genome and its relatively easy way to be transformed by both traditional methods or CRISPR transformation [1–3]. It was the first *Pooideae* genome to be entirely sequenced [4]. In recent years many studies provided new insight on the composition and structure of cell wall of various Brachypodium organs such as leaves, stem, sheath, root and embryo [5–7]. Brachypodium has a chemical composition similar to that of other important forage grasses with respect to major constituents, lignins, hydroxycinnamates, polysaccharides and proteins.

Recently, descriptions and comparative views of grain development of the reference accession of Brachypodium Bd21 highlighted Brachypodium as an intermediary in many respects between Triticeae and rice [8–11]. Brachypodium plant forms a caryopsis with an adherent pericarp. Around three days after flowering (DAF), the grain mainly consists of maternal layers surrounding the central cell in which the endosperm developed [11]. Together with the degeneration of maternal tissues, the endosperm developed until being fully cellularized at approximately 10 DAF. The endosperm cells expanded to reach the nucellar epidermis that corresponds to the innermost cellular layer of the outer layers. At this stage, the grain reaches its maximum length (7-8 mm). The endosperm cell walls start to thicken until the maturation of the grain.

The Brachypodium grain dimension is closely related to *Elymus* and *Bromus* genera and some wild wheats [8]. It is comparable in length with that of cultivated wheat, but dramatically contrasts in terms of width and depth, the grain of wheat having more rounded profiles. The grain of Brachypodium has a prominent and persistent nucellar epidermis and from this point of view is intermediate between rice and wheat [12]. The aleurone cells of Brachypodium grain are characterized by an irregular and poor organization forming one to three or more layers, and fused to the central endosperm. This layer is involved as a major transfer tissue in wheat [13]. For Brachypodium grain, an alternative transport of nutrients may exist via the persistent nucellar epidermis, as proposed for rice [8,14,15].

111 Like other grains of Poaceae, the both major hemicelluloses that compose the cell walls of
112 Brachypodium grain are feruloylated arabinoxylans and mixed linked β-glucan (MLG).
113 Despite similar arabinoxylan content, the ratio of ferulic acid to arabinoxylan is particularly
114 high when compared to wheat and barley. Brachypodium grains are also characterized by
115 high cellulose content relative to pectin and mannan [9]. The endosperm of Brachypodium
116 grains possesses thick cell walls rich in MLG. The unusually high MLG content of
117 Brachypodium (45% w/w ; [11]) contrasts with cereals and most wild grasses, where the
118 highest β-glucan contents among cereal grains are found in barley and oats (4–10%, w/w)
119 [16]. The nucellar epidermis contains a large amount of MLG and the thickness of the cell
120 walls in this tissue suggests they may also contribute to this tissue resistance to deformation
121 [8]. In addition to its structural role, MLG could act as a storage carbohydrate mobilized
122 during germination to supplement the low starch content of Brachypodium grain [8,10].

123 Although the cell wall composition of endosperm has been largely described in the mature
124 grain of Brachypodium [8,10], few data on the change of polysaccharide distribution in the
125 endosperm as well as in the outer layers are available on the course of grain development.
126 These data would be critical to understand the dynamic of cell wall assembly and to rely
127 them to the developmental processes of grain. Recently we considered the cell wall
128 proteome of Brachypodium grain at several developmental stages [17,18] and about 300 cell
129 wall proteins were identified as potentially involved in the construction and remodeling of
130 the cell wall. Among them, numerous glycosyl hydrolases, expansins and peroxidases were
131 identified. This work allowed a better understanding of the dynamic of cell wall remodeling
132 in the Brachypodium grain. However, data from polysaccharide composition and structure
133 are still lacking to highlight the process of cell wall implementation and remodeling during
134 grain development.

135 In this study we investigated the cell wall polysaccharide distribution during grain
136 development of Brachypodium from the end of the cellularization stage until the late
137 maturation stage. The distribution of polysaccharides was observed both in the endosperm
138 and the outer layers, asking questions about the role of the different polysaccharide families
139 during grain development.

140

141 ## 2. Materials and methods

142 ### 2.1. Materials

143 #### 2.1.1. Plant materials

144 *Brachypodium distachyon* line Bd21 was grown at temperatures of 24°C day/18°C night with
145 a photoperiod of 20 h light/4 h dark. Grains were harvested at several developmental stages
146 between 8 and 41 days after flowering (DAF) (8, 14, 19, 23, 41 DAF). For further biochemical
147 analyses, the endosperm and the outer layers were separated by hand and they were
148 immediately frozen in liquid nitrogen, freeze-dried, and crushed in powder as well as whole
149 grains.

150 #### 2.1.2. Enzymes

151 Enzymes were purchased from Megazyme (www.megazyme.com): Endo-1,4-β-D-Xylanase
152 M1 from *Trichoderma viride* and Lichenase were used for pretreatment of grain section
153 before immunolabeling, while recombinant Endo-1,4-β-D-Xylanase from *Neocallimastix*
154 *patriciarum* (Endoxylanase NP) was used for fingerprinting analyses.

155 #### 2.1.3. Antibodies

156 Rat monoclonal antibodies, LM20, LM19, LM5, LM6, LM21, LM25 as well as CBM3a were
157 obtained from Dr J.P. Knox (Centre for Plant Science, School of Biochemistry and Molecular
158 Biology, Leeds University, England). The mouse monoclonal antibody MLG was purchased
159 from Biosupplies Australia (http:// www.biosupplies.com.au). The mouse monoclonal
160 antibodies INRA RU1 (RU1), and INRA AX, the rabbit polyclonal antibody FerAra were
161 produced in our laboratory [19–21]. Specificities and references of antibodies are
162 summarized in Table 1.

163

164

165

166

167 **Table 1**
168 Antibodies and carbohydrate-binding module used in this study.

Antibodies/CBM	Antigen	References
Anti-AX1	Unsubstituted or low substituted arabinoxylan	[20]
Anti-5-O-Fer-Ara	5-O-(trans-feruloyl)-L-arabinose	[21]
MLG	Mixed link β-glucan	[22]
LM19	Unesterified homogalacturonan	[23]
LM20	Methyl-esterified homogalacturonan	[23]
LM21	Heteromannan	[24]
LM25	Xyloglucan	[25]
RU1	Rhamnogalacturonan	[19]
LM5	(1-4)-β-D-galactan	[26]
LM6	(1-5)-α-L-arabinan	[27]
CBM3a	Cellulose	[28]

169

170 2.1.4. Secondary antibodies

171 Goat anti-rat, anti-mouse and anti-rabbit-IgG conjugated with ALEXA Fluor 546 were
172 obtained from Molecular Probe, Oregon (USA). Nanogold conjugates and silver
173 enhancement kit were obtained from Aurion (NL).

174 **2.2. Methods**

175 2.2.1 Histochemistry

176 Grains at different developmental stages were fixed overnight in 3% (w/v) paraformaldehyde
177 in 0.1M phosphate buffer, pH7.4 dehydrated in ethanol series, and embedded with LR-White
178 resin as described by Chateigner-Boutin et al. [29].

179 Transverse semi-thin sections (1µm) of grains were cut with an ultracut (UC7, Leica) and
180 stain either with Toluidine Blue O (1% in 2.5% Na_2CO_3 for 5 min then washed in water) or
181 Sudan Red (1% in P20 polyethylene glycol to reveal the cuticles for 20 min, then washed in
182 ethanol 70%) or Acridine Orange (0.02% in sodium phosphate buffer 0.1M à pH7.2 for 15
183 min then washed in water). Stained sections were observed using a Multizoom Macroscope
184 (AZ100M, Nikon) under bright-field conditions for Toluidine Blue and Sudan Red. Acridine

185 Orange sections were imaged under epifluorescence irradiation using a band-pass filter
186 (461-489nm) and fluorescence detection above 515nm.
187
188 2.2.2. Immunolabeling (fluo and MET)

189 The grain sections were pre-treated with Lichenase and Xylanase to remove (1–3) (1–4)-β-
190 glucan (MLG) and arabinoxylan (AX) and observe the presence of cellulose, pectin, mannan,
191 and xyloglucan in cell walls. Sections were incubated with Lichenase (1.4U/50µl) and
192 desalted Endo-Xylanase M1 (0.8U/50µl) in water at 40 °C, overnight for immunofluorescence
193 or for 4h for transmission electron microscopy (TEM). Then, the sections were rinsed
194 thoroughly with de-ionized water. To observe the presence of AX, the grain sections were
195 only pre-treated with Lichenase.

196 Grain sections were successively incubated at room temperature in a blocking solution (3%
197 (w/v) bovine serum albumin (BSA), 0.1 M Na-phosphate buffer saline (PBS), pH 7.2) for
198 30 min and in solutions containing primary antibodies for 1 h. The dilutions of the antibodies
199 in PBS containing 1% (w/v) BSA and 0.05% (w/v) Tween-20 were: 1:20 for anti-AX1, 1:200 for
200 anti-(1–3) (1–4)-β-glucan, 1:2000 for anti-5-O-Fer-Ara, 1:10 for LM5, LM6, and 1:5 LM21 and
201 LM25.

202 For transmission electron microscopy observations, the ultra-thin sections (80nm)
203 extensively washed with buffer were incubated for 1 h in a solution containing the secondary
204 antibody at a dilution of 1:20 (v/v). Secondary antibodies were conjugated with 1 nm
205 colloidal gold complexes (Aurion, www.aurion.nl). The sections were then washed with PBS
206 and water. The gold particles were intensified by homogenous deposition of metallic silver
207 (Aurion, www.aurion.nl). The ultra-thin sections were examined with a transmission electron
208 microscopy (1230, Jeol) with an accelerating voltage of 80 KeV.

209 For immunofluorescence labeling, the semi-thin sections (1µm) were treated following the
210 same procedure described above using Alexa 546-conjugated secondary antibody (Molecular
211 Probes, www.invitrogen.com) diluted in PBS [1:100 (v/v)] for 1 h. The sections were
212 observed with a microscope (DMRD, Leica) equipped with epifluorescence irradiation. A

213 band-pass filter 515–560 nm was used as excitation filter and fluorescence was detected at
214 >590 nm.

215 2.2.3. Fingerprinting

216 Cell walls from freeze-dried powder of whole grain and the hand separated endosperm and
217 outer layers were prepared as alcohol insoluble material (AIM) as previously described [10].
218 The alcohol insoluble material (2 mg for 8 DAF samples and 8 mg for others samples) were
219 suspended in 0.4 ml of water and digested overnight (16h) at 40 °C under stirring with 5 U of
220 Endoxylanase NP. The reaction mixture was boiled for 10 min to inactivate the enzyme. After
221 cooling, the reaction mixture was centrifuged (10 000 *g*, 15 min) and the supernatant was
222 recovered and filtered on a 0.45µm membrane prior to chromatographic analysis.

223 Separation of Arabino-Xylo-OligoSaccharides (AXOS) from endoxylanase supernatants was
224 carried out with a high-performance anion-exchange chromatography system (ICS-5000
225 Pump and Ultimate 3000 Auto-Sampler; Thermo-Fisher Scientific, MA, USA) with pulsed
226 amperometric detection (HPAEC-PAD; ED50 Electrochemical Detector, Dionex, Sunnyvale,
227 USA). 5 µl of enzymatic digests were injected on a CarboPac™ PA200 analytical column
228 (3x250mm, Thermo-Fisher) equipped with a CarboPac™ PA200 guard column (3× 50mm,
229 Thermo-Fisher) eluted at a flow rate of 0.4 $ml.min^{-1}$ and maintained at 25 °C.

230 Mobile phases were prepared in degazed utrapure water with helium sparging. They were
231 composed of solvant: A (100% ultrapure water), B (1M NaOAc) and C (0.5M NaOH). The
232 gradient consisted of using 20% of C and a linear increase from 0% to 17% of B in 30 min,
233 followed by a rapid decrease to 0% B within 1 min. Composition was maintained at 20% of C
234 for 30 min for re-equilibration of the column.
235 AXOS were identified using the nomenclature of Fauré el al. [30] on the basis of their
236 retention times by comparison with standard mixture of AXOS obtained from enzymatic
237 hydrolysis of purified wheat AX [31,32].
238

239 2.2.4. Chemical analyses

240 All measurements were performed in duplicate on dry samples. Neutral sugar content and
241 composition of polysaccharides were determined by gas chromatography after acid
242 hydrolysis and conversion of monomers into alditol acetates as described in Dervilly *et al.*

243 (2000)[33]. Starch glucose was quantified by HPAEC (PA1 column 250 × 4 mm, Dionex,
244 Sunnyvale, CA, USA) after amylolysis [34]. The acetyl contents were measured in duplicate
245 by HPLC after alkaline hydrolysis by HPLC on a C18 column (4x 250 mm) eluted with 4 mM
246 H_2SO_4 at 0.7 ml/min and 25°C with refractometric detection [35].

247

248 **3. Results and discussion**

249 ***3.1. Morphology of grain***

250 Grains were harvested between 8 days until 41 days after flowering (DAF) in order to
251 analyse Brachypodium grain at the main crucial steps of development from the end of
252 cellularization until the maturation stages (Fig. 1A). At 8 DAF, the grain of Brachypodium
253 reaches around the half of the palea [18]. The cells of the fully cellularized endosperm
254 continue to expand and have thin cell walls. At this stage, the outer layers are well
255 developed and easily distinguishable, with an extensive nucellar epidermis, testa (inner
256 and outer teguments), and pericarp (tubular and transverse cells, outer pericarp).
257 Gradually maternal tissues degenerate resulting in a decrease of the outer layers
258 thickness during the following developmental steps of grains (Fig. 1B). Meanwhile, the
259 endosperm cells continue to divide and the grain expands as the same time as it
260 lengthens. From 14 DAF the aleurone cells are well recognizable at the peripheral of the
261 endosperm. Until the maturation step, cell walls gradually thicken, storage proteins and
262 starch accumulate into the endosperm cells (Fig. 1A,B ; [11]). In parallel to grain
263 development, the embryo completes its morphogenesis until the endosperm has
264 reached its final size [11]. Two cuticles present from the early stage frame the testa: one
265 of them is found between the t2 layer of the testa and the tubular and transverse cell
266 layer; the second, thinner, separates the pigmented cells of the testa (t1 layer) from the
267 nucellar epidermis (Fig. 1C). A similar structure of the testa surrounded by cuticles was
268 previously described in barley and wheat [36,37]. A thick cuticle tightly associated with
269 the outer side of the mature endosperm and acting as a barrier surrounding and isolating
270 the seed's living tissues was recently described in mature Arabidopsis seeds [38,39]. 3.2.

271 **3.2. *Carbohydrate composition***

272 Carbohydrate composition of polysaccharides was determined from the alcohol insoluble
273 fractions of the whole grain at four developmental stages (Table 2A).

274 **Table 2**
275 Sugar composition of the alcohol insoluble material (AIM) prepared from whole grain (A), endosperm
276 (B) and outer layers (C) of Brachypodium during grain development.

A

Sugars (% weight)	whole grain 8 DAF		whole grain 20 DAF		whole grain 28 DAF		whole grain 38 DAF	
	means	standard deviation	means	standard deviation	means	standard deviation	means	standard deviation
Rhamnose	**0,30**	0,04	**0,31**	0,05	**0,28**	0,00	**0,26**	0,02
Arabinose	**2,29**	0,465	**2,39**	0,05	**2,52**	0,08	**2,23**	0,00
Xylose	**2,09**	0,01	**2,69**	0,01	**3,33**	0,22	**3,05**	0,00
Mannose	**0,33**	0,045	**0,29**	0,11	**0,10**	0,01	**0,10**	0,04
Galactose	**0,76**	0,045	**0,78**	0,02	**0,54**	0,08	**0,54**	0,07
Glucose (total)	**42,06**	0,795	**57,12**	1,74	**57,30**	2,30	**54,46**	0,93
starch	**4,26**	0,05	**4,12**	0,12	**3,49**	0,17	**3,57**	0,31
Ratio A/X	**1,09**		**0,89**		**0,76**		**0,73**	
Sum A+X	4,38		5,08		5,85		5,28	
Total sugars	**47,81**		**63,60**		**64,13**		**60,68**	
Acetylation	nd		**0,366**	0,02	**0,360**	0,04	**0,307**	0,09

277

B

sugars (% weight)	endosperm 20 DAF		endosperm 28 DAF		endosperm 38 DAF	
	means	standard deviation	means	standard deviation	means	standard deviation
Rhamnose	**0,25**	0,01	**0,30**	0,05	**0,21**	
Arabinose	**1,76**	0,03	**1,66**	0,01	**1,68**	
Xylose	**1,79**	0,02	**1,66**	0,01	**1,48**	
Mannose	**0,20**	0,12	**0,16**	0,04	**0,00**	
Galactose	**0,69**	0,04	**0,48**	0,03	**0,43**	
Glucose	**54,67**	1,67	**55,76**	0,25	**55,25**	
Ratio A/X	**0,99**		**1,00**		**1,14**	
Sum A+X	3,55		3,32		3,16	
Total sugars	**59,39**		**60,05**		**59,05**	

278

C

sugars (% weight)	outer layers 20 DAF		outer layers 28 DAF		outer layers 38 DAF	
	means	standard deviation	means	standard deviation	means	standard deviation
Rhamnose	**0,30**	0,01	**0,32**	0,01	**0,28**	0,01
Arabinose	**3,53**	0,01	**4,10**	0,09	**4,17**	0,07
Xylose	**5,16**	0,06	**8,07**	0,11	**7,96**	0,10
Mannose	**0,40**	0,21	**0,12**	0,06	**0,16**	0,07
Galactose	**0,68**	0,05	**0,61**	0,10	**0,30**	0,25
Glucose	**69,84**	0,37	**63,72**	0,86	**63,21**	0,02
Ratio A/X	**0,68**		**0,51**		**0,52**	
Sum A+X	8,69		12,16		12,13	
Total sugars	**80,10**		**77,06**		**76,21**	

279

280 The total carbohydrate content ranged between 47% and 60% depending on the grain stage,
281 the remnant being mostly proteins and fatty acids according to previous works [11]. Among
282 total carbohydrate, starch represented around 4% of the fresh weight that is consistent with
283 the low starch content of Brachypodium grain [11,40]. We observed an increase of xylose
284 content leading to a decrease of the ratio arabinose/xylose, arabinose being relatively stable
285 during whole grain development. Xylose and arabinose residues mainly derive from
286 arabinoxylans, one of the major components of Brachypodium cell walls. To lesser extent
287 arabinose might also derive from pectic rhamnogalacturonan I and arabinogalactans while
288 xylose residues could also arise from xyloglucan or pectic side chains. Mannose and
289 galactose amounts tended to decrease along whole grain development. These
290 carbohydrates are components of mannans, pectins and xyloglucan side chains. In addition,
291 the acetyl content decreased between 8 and 38 DAF, which can be related to the
292 identification of carbohydrate esterases by a proteomic approach ([18]; Table 3).

293 Brachypodium grains were hand dissected and the endosperm was separated from the outer
294 tissues in order to determine their individual carbohydrate composition (Table 2B and C).
295 The endosperm contained the aleurone cells and the storage endosperm, whereas the outer
296 layers included the nucellar epidermis, testa and pericarp. A clear difference in carbohydrate
297 composition was noticed between endosperm and the outer tissues. The total carbohydrate
298 content was higher in the outer layers compared to that of the endosperm. This was
299 probably due to the increasing amount of storage proteins accumulated in the endosperm
300 cells from 20 DAF until grain maturation [11]. Xylose and arabinose were two to three times
301 more abundant in the outer layers than in the endosperm, while rhamnose, mannose and
302 galactose amounts were close in the two grain parts. Glucose amount is particularly
303 abundant in the outer layers of Brachypodium grains, and strongly higher compared to those
304 of wheat [41]. This could be due to the persistence of a prominent nucellar epidermis that
305 characterizes Brachypodium grain.

306

307

308

309 **Table 3**

310 Proteins encoded by the family GT8 genes in Brachypodium plant (according to Yin et al., 2011 [42]
311 and completed by ProtAnnDB and PlaNet data).

312

Accession number	GT8 Clade/subclade (Yin et al., 2011)	Annotation (according to ProtAnnDB)	Loc Tree	Nb TM domains (tmhmm)	Pfam	Transcript expression in grain #
Bradi1g60010.1	GAUT/GAUTc	galacturonosyltransferase 11	golgi apparatus membrane	1	PF01501 GT 8	+
Bradi5g23250.2	GAUT/GAUT-c	galacturonosyltransferase 10	golgi apparatus membrane	2	PF01501 GT 8	+/-
Bradi3g20550.1	GAUT/GAUT-e	galacturonosyltransferase 4	golgi apparatus membrane	1	PF01501 GT 8	+
Bradi3g39270.1	GAUT/GAUT-e	galacturonosyltransferase 4	golgi apparatus membrane	1	PF01501 GT 8	+ *
Bradi4g33280.1	GAUT/GAUT-e	galacturonosyltransferase 4	golgi apparatus membrane	1	PF01501 GT 8	+
Bradi3g43810.1	GAUT/GAUT-b	Nucleotide-diphospho-sugar transferases superfamily protein	golgi apparatus membrane	1	PF01501 GT 8	+
Bradi3g59370.1	GAUT/GAUT-b	Nucleotide-diphospho-sugar transferases superfamily protein	golgi apparatus membrane	1	PF01501 GT 8	+
Bradi4g36050.1	GAUT/GAUT-d	galacturonosyltransferase 1	golgi apparatus membrane	1	PF01501 GT 8	
Bradi1g70290.1	GAUT/GAUT-a	galacturonosyltransferase 14	golgi apparatus membrane	1	PF01501 GT 8	+/-
Bradi1g63520.1	GAUT/GAUT-g	galacturonosyltransferase 7	golgi apparatus membrane	1	PF01501 GT 8	+
Bradi4g03670.1	GAUT/GAUT-a	galacturonosyltransferase 13	golgi apparatus membrane	1	PF01501 GT 8	+/-
Bradi1g45210.2	GAUT/GAUT-b	Nucleotide-diphospho-sugar transferases superfamily protein	golgi apparatus membrane	1	PF01501 GT 8	+
Bradi1g29784.1	GAUT/GAUTc	galacturonosyltransferase 3	golgi apparatus membrane	1	PF01501 GT 8	+
Bradi1g12180	GAUT/GAUT-d	galacturonosyltransferase 1	golgi apparatus membrane	0	PF01501 GT 8	+
Bradi4g14910.1	GAUT/GAUT-f	galacturonosyltransferase 6	golgi apparatus membrane	1	PF01501 GT 8	+
Bradi1g17570.1	GAUT/GAUT-g	galacturonosyltransferase 7	golgi apparatus membrane	1	PF01501 GT 8	++ *
Bradi3g61120.1	GAUT/GAUT-g	galacturonosyltransferase 7	golgi apparatus membrane	0	PF01501 GT 8	+ *
Bradi4g44070.1	GAUT/GAUT-g	galacturonosyltransferase 7	golgi apparatus membrane	1	PF01501 GT 8	+
Bradi5g12290.1	GAUT/GAUT-g	galacturonosyltransferase 7	golgi apparatus membrane	0	_	nd
Bradi1g29784.1	nd	galacturonosyltransferase 3	golgi apparatus membrane	1	PF01501 GT 8	+
Bradi1g44470.1	GATL-a	glucosyl transferase family 8	endoplasmic reticulum membrane	0	PF01501 GT 8	-
bradi3g59760.1	GATL-a	glucosyl transferase family 8	endoplasmic reticulum membrane	1	PF01501 GT 8	+/-
Bradi1g64830.1	GATL-b	galacturonosyltransferase-like 7	endoplasmic reticulum membrane	0	PF01501 GT 8	-
Bradi1g12560.1	GATL-c	galacturonosyltransferase-like 2	endoplasmic reticulum membrane	1	PF01501 GT 8	nd
Bradi5g16690.1	GATL-d	galacturonosyltransferase-like 4	endoplasmic reticulum membrane	0	PF01501 GT 8	+/-
Bradi1g61830.1	GATL-e	galacturonosyltransferase-like 4	endoplasmic reticulum membrane	1	PF01501 GT 8	+
Bradi1g06917.1	nd	galacturonosyltransferase-like 7	secreted	0	PF01501 GT 8	+

313 # : expression level of corresponding transcripts according to the data available from PlaNet
314 (http://aranet.mpimp-golm.mpg.de/). * : transcripts more expressed in endosperm and whole grain
315 compared to others tissues/organs.

316

317 The ratio arabinose to xylose tended to increase in the endosperm during grain development
318 while it decreased in the outer layers and ended up with a value twice as low as that of the
319 endosperm. If we assume that these two sugars mainly arise from arabinoxylan, the values
320 suggest that arabinoxylans into the endosperm cell walls are more substituted than those in
321 the outer layers. However, as mentioned above, we have to keep in mind that these two
322 sugars may also contribute to pectic, arabinogalactan and xyloglucan composition present in
323 low amount in Brachypodium grain. The ratio arabinose to xylose is lower in Brachypodium

324 compared to that of wheat outer layers during grain development [41]. In addition, the
325 substitution degree of AX varies according to the outer layer tissues in wheat, with a low A/X
326 ratio in the nucellar epidermis and a higher ratio in the outer pericarp, this latter being about
327 50% of outer layers in wheat [43]. The prevalence of outer pericarp in wheat grain and as
328 counterpart, a particularly well developped nucellar epidermis in Brachypodium, could
329 explain the highest A/X ratio in wheat outer layers compared to that in Brachypodium.

330 As expected, the different carbohydrate composition and evolution during grain
331 development clearly traduces distinct cell wall dynamics in the two parts of the grains, which
332 could be related to their function.

333 The fine structure of arabinoxylan in developing grains was further investigated by
334 enzymatic fingerprinting (Fig. 2). The alcohol insoluble material (AIM) derived from whole
335 grain or isolated endosperm or outer layers of grain harvested at different stages of
336 development were treated with an endoxylanase and degradation products were submitted
337 to HPAEC analysis.

338 Considering the whole grain, the main oligosaccharides identified at 20 and 38 DAF are:
339 XA3XX, XA2+3XX, XA3A3XX, XA3XA3XX, XA3A2+3XX and XA2+3A2+3XX, together with the
340 unknown oligosaccharides UX1, UX5 and UX6 already found in wheat [10,31] (Fig. 2A). In
341 addition, three supplementary oligosaccharides were eluted at 13.3, 22.1 and 29.9 min that
342 seems specific to Brachypodium xylan hydrolysate. The arabinoxylan enzymatic profiles
343 appeared similar between the stages 20 and 38 DAF, however a significant decrease of all
344 peak areas was observed for the older stage. The lower release of oligosaccharides from
345 later stage grains suggests a more difficult degradation of AX by the endoxylanase, probably
346 in connexion with lignin, ferulic acid dimerization and tight interactions between
347 hemicelluloses and cellulose microfibrils. The xylan profile obtained from the whole grain at
348 the early stage (8 DAF) was quite different. Whereas additional oligosaccharides appeared
349 (XXA3XX and an unknown peak eluted at 12,8 min), some oligosaccharides identified at later
350 stages (UX1 and XA2+3A2+3XX) were not detected. In addition, the xylose was quite
351 abundant compared to the other stages. Whereas the predominant oligosaccharides
352 corresponded to XA3XX, XA2+3XX and peak at 22.1 min for the 20 and 38 DAF hydrolysates,

353 the most abundant oligosaccharides found at 8 DAF were still no identified (UX5, UX6 and
354 peaks at 12,8 and 22.1 min).

355 The sugar composition suggests difference in the chemical structure of AX in the outer layers
356 and in the endosperm. To go further in the exploration of the fine structure of AX according
357 to grain parts, AX enzymatic fingerprinting was applied to hand dissected material (Figure
358 2B). The endoxylanase digestion released well identified xylose oligosaccharides until DP4
359 from the outer layers whereas only xylose (X1) and xylobiose standed out from the
360 endosperm samples. In the outer layers hydrolysate, XA3XX is the main arabino-xylo-
361 oligosaccharide whereas this latter is in lower abundance in the endosperm hydrolysate but
362 with the prevalence of XA2+3XX oligosaccharides. This result might indicate the presence of
363 more substituted arabinoxylans in endosperm than in the outer layers, and corroborates the
364 result of a higher ratio of arabinose to xylose observed in the endosperm (Table 2). The peak
365 at the retention time of 13,3 min seems specific to the endosperm samples. As already
366 noticed in the whole grain‘s fingerprinting, we pointed out the presence of the unknown
367 peak at a retention time of 22.1 min in both endosperm and outers layers compartments
368 and the global decrease of all xylo-oligosaccharides abundance throughout the grain
369 maturation. Arabinoxylan enzymatic fingerprints of the developing endosperms are similar
370 to that of the endosperm in mature dry grain reported by Guillon et al. (2011) [10] with the
371 detection of XA3XX and XA2+3XX as major oligosaccharides. In addition, the peaks eluted at
372 13.3 and 22.1 min seem to correspond to those previously identified in the endosperm of
373 mature dry grain and named UXbra1 and UXbra3 respectively. Moreover the area of the
374 arabino-xylo-oligosaccharides peaks were significantly lower in mature grain chromatogram
375 compared to those of endosperm of developing grain, which is consistent with our
376 observation of a global decrease of xylo-oligosaccharides abundance throughout the grain
377 maturation.

378 The enzymatic fingerprint data showed a clear structural variation of arabinoxylan between
379 endosperm and the outer layers of Brachypodium grain, as well as between the early
380 developmental stage and the latter ones. Further analysis by mass spectroscopy is required
381 to identify the unknown oligosaccharides and to further decipher changes in the fine AX
382 structure between endosperm and outers layers during grain development.

383 By proteomic, arabinofuranosidases belonging to the GH51 family were specifically
384 identified at 19 DAF of Brachypodium grain but not at earlier stages [18]. The higher amount
385 of GH51 at 19 DAF was suggested to be related to the debranching of AXs during the
386 development of the Brachypodium grain. This suggestion is supported by our results
387 showing a strong release of the UX5 and UX6 oligosaccharides in the 8 DAF hydrolysate while
388 they were almost non-existent at 20 and 38 DAF (Fig. 2A). Indeed, based on their retention
389 times, these xylo-oligosaccharides should indicate the presence of more highly substituted
390 arabinoxylan at 8 DAF than at later stages.

391

392 ### *3.3. Carbohydrate distribution during grain development*

393 To investigate the distribution of polysaccharides all along the development of
394 Brachypodium grain, immunolabelings were performed using carbohydrate-binding module
395 and antibodies directed to the cell wall matrix polysaccharides (Table 1). Except for
396 immunolabeling with MLG antibodies, a pre-treatment with lichenase and xylanase was
397 applied on grain sections to increase the labeling detection of polysaccharides [10]. For
398 immunolabeling with AX antibodies, only lichenase pre-treatment was applied.
399 Autofluorescence sometimes interferes with the immunofluorescence signal, especially for
400 low abundant polysaccharides. Plant cell wall autofluorescence is mainly linked to the
401 presence of phenolic compounds such as lignin and hydroxycinnamic acids (ferulic acid,
402 para-coumaric acid, etc.), as demonstrated in wheat peripheral tissues [44].
403 Autofluorescence can also be introduced by fixatives [45]. In Brachypodium grain, the
404 occurrence of lignins was recently established in the outer layer of the testa (t2) [46]. Here
405 we observed autofluorescence mainly in the t1 layer of the testa, which was probably due to
406 the strong abundance of pigments into these cells (Fig. 1; Fig.S1). In addition to
407 immunofluorescence, immunogold labeling and observation by electronic transmission was
408 carried out to confirm some results.

409 #### *3.3.1. Arabinoxylans*

410 Arabinoxylans (AX) are one of main polysaccharides in Brachypodium grains. The deposition
411 of AX in starch endosperm and outer layers was investigated in several cereal species such as

412 barley, wheat or rice [15,47,48] but not yet in Brachypodium grain. Immunolabeling of the
413 nucellar epidermis's cell walls with INRA AX1 is high at the early developmental stage but
414 decreased from 19 DAF to the maturation (Fig. 3A). A low labeling was observed in the
415 external pericarp whatever the developmental stage. In the testa a faint labeling was
416 observed from the early stage by immunofluorescence, which was confirmed using electron
417 microscopy (Fig. 7). In contrast, immunolabeling in the endosperm and in the aleurone cell
418 walls increased all along the development (Fig. 3A,B).

419 Arabinoxylans in Brachypodium appear to be highly feruloylated [10]. The whole grain of
420 Brachypodium contains twice the amount of monomeric ferulic acid of the wheat grain (1.7
421 mg/g vs 0.9 mg/g of whole grain) [10,43,46]. A high fluorescence with an antibody directed
422 against feruloylated arabinoses (Fer-Ara antibodies) was found in the nucellar epidermis of
423 grain at early developmental stages, as well as in the testa (Fig. 3A and 7). High level of
424 ferulic acid was previously reported in outer layers of mature grain of Brachypodium [10]. In
425 wheat, high fluorescence was also found in the nucellar epidermis and the testa at early
426 developmental stages [21]. The high immunofluorescence labeling in the storage endosperm
427 cell walls compared to that observed in the aleurone cell walls at 14-19 DAF, confirmed by
428 immunogold labeling, suggest a faster feruloylated arabinoxylans accumulation in the
429 storage endosperm (Fig. 3B). This result is in contrast with those previously observed in
430 wheat, where Fer-Ara epitopes were also detected in cell walls of starchy endosperm, but at
431 a lower level than in aleurone [21].

432 ***3.3.2. Mixed linked β-Glucan***

433 MLG is the most abundant polysaccharides of Brachypodium grain and is enriched in 1→3
434 linkages compared to other grasses [10,16]. The spatial distribution of MLG in developing
435 grain was examined by fluorescent microscopy using specific antibodies. An intense
436 fluorescence was observed at the early stage (8 DAF) and until the 19 DAF in the outer layers
437 including epidermis nucellar, testa and pericarp (Figure 4). At latter stages, the accumulation
438 of MLG was still observed in the nucellar epidermis and testa. In wheat, MLG are detected at
439 the early stage in the nucellus epidermis but then decrease as the grain mature at the
440 expense of xylans [49]. MLG labeling was observed in the endosperm cell walls all along the
441 grain development (8-41 DAF), highlighting an accumulation of the polysaccharide according

442 to the cell wall thickening. A similar pattern of MLG was previously described in developing
443 grain of the Brachypodium line Bd21 [11]. The high amount of MLG not only in the
444 endosperm as already highlighted by Guillon et al. [11], but also in the outer layers and in
445 particular in the nucellus epidermis, questions about its dual role as structural and storage
446 polysaccharides in these different tissues of the grain .

447 ***3.3.3. Cellulose***

448 Cellulose was visualized in the developing grain using the carbohydrate-binding module
449 CBM3a. The CBM3a has been suspected to bind xyloglucan in addition to cellulose [50].
450 However, recent investigation demonstrated that this carbohydrate-binding module binds
451 only aggregated regions of xyloglucan found in solution and not xyloglucan oligosaccharides,
452 then confirming the usefulness of CBM3a as a selective probe for cellulose embedded in the
453 cell wall [51].

454 Cellulose was detected at early developmental stage of Brachypodium in nucellar epidermis
455 and external pericarp, but nor in the pericarp parenchyma or in the testa (Fig. 4). No
456 cellulose was visualized in endosperm cells at 8 DAF, but the increase of labeling from 14
457 DAF until the mature stages suggests a progressive accumulation. Although the aleurone
458 cells reacted with the affinity probe, the immunofluorescence was very low compared to
459 that of the endosperm cells. This observation is in agreement with previous data obtained by
460 FTIR spectroscopy in mature grain and reported by Guillon et al. [10]. In wheat, Gartaula et
461 al. [52] demonstrated that cell walls of pure endosperm tissue contain a significant
462 proportion of cellulose (ca 20%) higher than reported for long in wheat white flour. As in
463 Brachypodium grain, cellulose was relatively evenly distributed across the storage
464 endosperm. The authors suggest that cellulose associates with xylans and heteromannans to
465 form a resistant network that may be responsible for the structural integrity of the
466 endosperm cell walls.

467 ***3.3.4. Other hemicelluloses***

468 ***3.3.4.1. Mannans***

469 Mannans were previously revealed at a low amount in the endosperm cells of mature grain
470 of Brachypodium [10]. Recently, mannans were also detected in the Brachypodium embryo

471 [7,53]. Here we detected mannans in endosperm cells from 19 DAF to the maturation stage
472 with no or very low fluorescence detection in the aleurone cells (Fig. 4). In the outer layers,
473 faint fluorescence was observed in the epidermis nucellar until the 19 DAF, and in the
474 pericarp cells. In the t1 layer of the testa, we suspected that the signal corresponded to
475 autofluorescence of native compounds. Indeed, compared with other antibodies used,
476 visualization of immunolabeling with LM21 required a long acquisition time (Figure 4). A
477 similar deposition was observed in the grains of wheat and barley, with the immunolabeling
478 of the starchy endosperm as well as the outer layers (nucellar epidermis and pericarp) and
479 only a weak immunolabeling in the aleurone of developing grain but no at maturity [15,54–
480 56]. By contrast, no mannans were detected in endosperm cell walls of rice at any
481 developmental stage, although they were observed in the outer maternal tissues [15].

482 ***3.3.4.2. Xyloglucans***

483 Using the specific antibody LM25, we visualize the presence of xyloglucan in the outer layers,
484 especially in the epidermal cells and in the testa all along the grain development (Fig. 4; Fig.
485 7A,B). Using LM15 antibody, Guillon et al. [10] were not able to detect them in the mature
486 grain. Because of a long exposure time for image acquisition, the fluorescence detected in
487 the t1 layer of the testa might correspond to autofluorescence. However, a clear labeling
488 was detected by electron microscopy in the cuticle located above the t2 layer of the testa
489 (Fig. 7). Immunolabeling was also detected at a very low amount in the endosperm from 14
490 DAF with a decrease at 41 DAF, but not in the aleurone cells at any developmental stage. In
491 agreement with our observations, the presence of xyloglucan has been shown only in the
492 early stages in the endosperm of wheat and barley, but persists in the maternal outer tissues
493 over the grain development [15,54–56]. By contrast, xyloglucans was detected in the
494 aleurone of rice at later stages [15]. A recent study indicated the presence of xyloglucan in
495 the radicula and root cap of Brachypodium embryo which could play a significant role during
496 embryo development and seed germination [7]. To our knowledge, no detection of
497 xyloglucan in the cuticle of the testa layer was previously described in Poaceae grains.
498 Despite the low content of xyloglucan in the cereal cell walls, genome sequencing revealed
499 numerous sequences encoding putative xyloglucan endotransglycosylase/hydrolase (XTH)
500 belonging to the GH16 family and known to act on xyloglucan [57]. Proteomic analyses
501 confirmed the abundance of XTHs in the cell walls of Brachypodium grain [17,18]. The

502 contrast between xyloglucan content and related modifying enzymes abundance suggests
503 that some of them might be active on the major polysaccharides AX and MLG instead of
504 xyloglucan [58,59].

505 **3.3.5. Pectins : a specific deposition into the testa, pericarp and endosperm**

506 Pectins are classified into three major types, homogalacturonan (HG), rhamnogalacturonan-I
507 (RGI) and rhamnogalacturonan-II (RGII). rhamnogalacturonan I (RGI) is one of the most
508 heterogeneous polysaccharide found in plant cell walls. Its backbone is composed of
509 alternative rhamnose and galacturonic acid residues. RGI side chains include galactan,
510 arabinan and arabinogalactan. RGI side chain composition and structure are highly variable
511 and depend on species, organ, cell types and developmental stages [60,61].
512 Homogalacturonan (HG) comprises a backbone of α-(1–4)-linked D-Gal-A, which can either
513 be methylesterified at the C-6 carboxyl or carry acetyl groups at O2 or O3 [62,63]. RGII,
514 which is less abundant than the two others is a highly complex substituted HG, with up to six
515 different side-chain structures including at least twelve distinct monosaccharides.

516 The cell walls of the grass grain, and in particular of the endosperm, are known to have low
517 level of pectins compared to the cell walls of non gramineous plants [64]. Traces of pectins
518 were previously reported in the endosperm of mature grain of Brachypodium [10].
519 Surprisingly, numerous glycosyltransferases identified in the proteome of Brachypodium
520 were possibly involved in the synthesis of HG and RGI (Table 3). Here we investigated the
521 presence of RGI and HG in the developing grain thanks to antibodies.

522 By combining the use of three antibodies, INRA-RU1 specific for the RGI backbone, LM5 for
523 1,4 galactan, and LM6 for 1,5 arabinan, spatial differences in RGI motif distribution within
524 Brachypodium grain section was evidenced (Fig. 5). Maternal tissues were labeled with INRA
525 RU1 from 8 DAF. In the endosperm, the epitope was clearly observed from 23 DAF in the cell
526 walls of the aleurone layers. The nucellar epidermis was labeled with LM6 but only at the
527 earlier stage of grain development. No labeling with LM5 was observed. In the endosperm,
528 the galactan epitopes appeared restricted to the aleurone cell walls by 19 DAF while the LM6
529 epitope was observed in the cell walls of both the storage endosperm and the aleurone
530 layers by 14 DAF. This particular distribution pattern of pectin epitopes between storage
531 endosperm and aleurone layer was previously observed in developing grains of wheat

532 [15,29]. We also pointed out that immunolabeling with LM5 and LM6 revealed arabinan and
533 galactan in the cell walls nearby the plasma membrane in the aleurone and endosperm cells
534 (Fig. 5, higher magnification).

535 Low-methylated and methylated homogalacturonans were revealed using the LM19 and
536 LM20 antibodies respectively (Fig. 6). Homogalacturonans were detected all along the
537 development of the grain in the pericarp cell walls with a particular dot deposition at the cell
538 wall junctions. Whatever the antibodies used, no labeling was found in the aleurone cell
539 walls and only a faint one was detected in the endosperm. According to the electron
540 microscopy images, only a low labeling for methylated HG and no labeling for low-
541 methylated HG occurred in the cell wall of testa t2 layer at the early 8 DAF stage. At 14 DAF,
542 accumulation of homogalacturans was observed in the t2 cell layer of the testa. At 19 DAF,
543 both low-methylated and methylated homogalacturonans were visualized beneath the cell
544 wall of the t2 testa layer and also into vesicular bodies into the cytoplasm (Fig. 6A,B). Later in
545 development (41 DAF), LM20 epitopes was not anymore detected whereas a strong labeling
546 was revealed with LM19 (Fig. 6A,B). As already shown at 19 DAF, the labeling was restricted
547 to the area between the two cell walls of the t2 cell layer of the testa.

548 Pectin deposition was recently highlighted in the developing embryo of Brachypodium and in
549 the cells walls of wheat grain [7,29], this latter showing numerous similarities in the spatial
550 distribution of RGI and homogalacturonans with what we observed in the cell walls of
551 Brachypodium grain. For instance, the amazing localization of HG beneath the cell wall of the
552 testa and into vesicular bodies was noticed in wheat grain at the developmental stage of 250
553 days degree (°D), and the immunolabeling of the testa was detected only with LM19 at
554 750°D and not with LM20, but the intracellular location of low-methylated HG into the testa
555 was not specified at this developmental stage [29]. Apart our finding and those described in
556 wheat grain, homogalacturonans occurrence out of cell wall was described in fertilized ovule
557 cells of *Hyacinthus orientalis* L.**,** where HG are stored in the cytoplasm surrounding the
558 emerging endosperm cells, and may be used as a material for the construction of the
559 endosperm cell walls [65]. For now, we don't know the reasons why low-methylesterified
560 homogalacturonans were found out of the cell walls in the testa cell's layer of Brachypodium
561 grain.

562 Demethylesterification of HGs and/or a specific degradation of methylesterified HGs in this
563 cell layer may occur during the grain development. Homogalacturonans are probably highly
564 methyl-esterified when exported into cell walls and then is subsequently de-esterified in the
565 cell wall by the action of pectin methyl esterases (PMEs) [66,67]. Polygalacturonases (PG)
566 and pectin methyl esterases (PMEs) and other pectin degrading enzymes were annotated in
567 the cell wall proteome of the developing grain of Brachypodium ([18], summarized in Table
568 4). Their presence highlights possible important remodeling/degradation events of this class
569 of polysaccharides during the development of grain. Among them, one pectin methyl
570 esterase (PME; Bradi2g11860.1) was found to be more highly expressed at 19 DAF than at
571 earlier stages and could be involved in the demethylation events of homogalacturonans
572 during the development of Brachydodium grain.

573

574 **Table 4**
575 Proteins acting on pectins identified in the cell wall proteome of Brachypodium during grain
576 development (data from *Francin-Allami et al., 2016* [18]).
577

Accession number	Annotation (according to ProtAnnDB)		Loc Tree	Nb TM domains	Pfam	Relative abundance		
	functions	protein family		(tmhmm)		9 DAF	13 DAF	19 DAF
Bradi2g12047.2	PAE	carbohydrate esterase family 13	secreted	1	PF03283 PAE	-	+	+
Bradi2g12057.1	PAE	carbohydrate esterase family 13	secreted	0	_	+	+	+
Bradi5g20827.1	PAE	carbohydrate esterase family 13	secreted	1	PF03283 PAE	+++	++	+
Bradi2g11860.1	PME3	carbohydrate esterase family 8	secreted	0	PF01095/PF04043	++	+	+++
Bradi2g56820.1	Plantinvertase/ PMEi superfamily	carbohydrate esterase family 8	secreted	1	PF01095 PE	+	+	+
Bradi2g04550.1	polygalacturonase	glycoside hydrolase family 28	secreted	0	PF01095 PE	+	+	-
Bradi2g18030.1	polygalacturonase	glycoside hydrolase family 28	secreted	1	PF01095 PE	+	+	-
Bradi1g52050.1	polygalacturonase	glycoside hydrolase family 28	secreted	0	PF01095 PE	+	+	+
Bradi1g53430.1	polygalacturonase	glycoside hydrolase family 28	secreted	0	PF01095 PE	+	+	+
Bradi1g76890.1	polygalacturonase	glycoside hydrolase family 28	secreted	1	PF01095 PE	+	+	+
Bradi2g43750.1	polygalacturonase	glycoside hydrolase family 28	secreted	0	PF01095 PE	+	+	+
Bradi3g02850.1	polygalacturonase	glycoside hydrolase family 28	secreted	0	PF01095 PE	+++	++	+
Bradi4g05050.1	polygalacturonase	glycoside hydrolase family 28	secreted	0	PF01095 PE	+	+	+
Bradi4g11087.1	polygalacturonase	glycoside hydrolase family 28	secreted	0	PF01095 PE	+	+	+
Bradi4g33660.1	polygalacturonase	glycoside hydrolase family 28	secreted	0	PF01095 PE	+	+	+

578

579 Beside PME and PGs, arabinofuranosidases belonging to the GH51 family and GH35 β-
580 galactosidases were also identified in the proteome of Brachypodium developing grain and
581 might be also involved in the remodeling events of the RGI. However, neither potential
582 endo-arabinanase nor endo-galactanase belonging to the GH43 and GH53 families
583 respectively was identified [18]. In the same way, numerous remodeling enzymes potentially
584 involved in the degradation of pectins were also found in the cell wall proteome of wheat
585 grains (results to be submitted).

586 In agreement with these proteomic results, we showed that pectins, although minor
587 polysaccharides in Brachypodium grain, are relatively abundant in some tissues and have
588 undergone quite large structural changes during grain development. Our results show that
589 the structure of the RGI side chains differs according to the tissue in addition to the
590 developmental stage of Brachypodium grain, providing direct evidence of the dynamic
591 changes of pectin epitopes during the development of grain. Different population of RGI
592 molecules may be synthesized or remodeled *in muro* at different time during cell wall
593 development, which could explain the presence of numerous genes/proteins involved in the
594 biosynthesis and remodeling of pectin in Brachypodium grain (Tables 3 and 4). As previously
595 detected in wheat grain, HG was especially accumulated at the specific stage of 18-20 DAF in
596 the testa layers as vesicular bodies or secreted underneath the cell wall. This event might be
597 a feature shared by cultivated and wild poaceae grains. The reasons why homogalacturonans
598 are deposited into the cell content of the testa layer in a low-methylated form just before
599 the grain filling stage are still unknown. Further investigations should be led to understand
600 the role of this amazing spatial deposition of pectin in grain.

601 ***3.3.6. Focus on the polysaccharide distribution into the testa***

602 Our immunolabeling images using a panel of specific polysaccharides antibodies revealed a
603 particular distribution of some polysaccharides into the testa layers all along the
604 development of Brachypodium grain. As told above, the testa is composed of 2 layers of
605 cells, t1 and t2 and framed by two cuticles (Figure 1). Xyloglucan was only vizualized into the
606 cuticle above the t2 layer of the testa, and this, all along the developmental stages (Figure
607 7). The presence of polysaccharides associated to the cuticle was previously reported in
608 *Solanum lycopersicum* L. fruit, and was suggested confering stiffness and elastic properties

609 to the whole cuticle [68]. Although detected into the cuticle, feruloylated arabinoxylans
610 were mostly revealed into the cell wall of the testa with an evident polarity (Figure 7).
611 Indeed, AX1 and FerAra especially recognized epitopes into the cell walls of the t1 layer. This
612 distribution was observed from the early stage with a more pronounced polarity according
613 to the grain development. In the same way, a polarity of glucuronoxylan deposition was
614 observed in the testa of wheat grain at 250°D, where only one cell layer was immunolabeled
615 with antibodies specific to xylans (UX1 antibodies) [29]. As described for wheat [29],
616 homogalacturonans were detected in the cytoplasm of the t2 layer, and not into the cell
617 walls of the testa. The degree of methylesterification decreased as the grain aged.

618 To our knowledge, this is the first time that such a distribution of polysaccharides into the
619 testa including cuticles of Poaceae grain was reported. Our results question about why such
620 a peculiar polysaccharide distribution in the testa.

621

622 **4. Conclusion**

623 Although Brachypodium has been deeply studied for these latter years, especially the grain
624 at maturation, little information is known about the cell wall dynamics during the
625 development of grain. This work gives an overview of the composition and distribution of
626 the cell wall polysaccharides in Brachypodium grain from the cellularization step to the end
627 of grain filling. A schematic view of these results is represented in the Figure 8. Several
628 events are shared by the model plant Brachypodium and the wheat species, such as the
629 massive deposition of pectin as vesicular bodies in one of the testa layers, underneath the
630 cuticle. In addition, a polarized deposition of polysaccharides into the testa all along the
631 grain development suggests a specific role of this tissue during the grain growth.
632 Modifications of polysaccharide structures occur during grain development, such as
633 variations of the methylation degree of homogalacturonan or the arabinose substitution
634 degree of arabinoxylan.

635 Change in composition occurred in both the maternal tissues and endosperm all along the
636 grain development. Some connections have been made between these cell wall events and
637 several cell wall modifying-enzymes identified at different developmental stages of

638 Brachypodium grains by previous proteomic analyses. The relationship between these
639 structure variations and the remodeling enzymes will help to better understand the
640 dynamics of the cell walls in Poaceae plant and their role during the grain development, and
641 the impact in the final size and quality of grain.

642

643 **Acknowledgement**

644 This work was supported by INRA funding. We would like to acknowledge Axelle Bouder for
645 her contribution to the experimental analysis; Rémi Gardet and Daniel Sochard (Angers,
646 IRHS, INEM platform) for Brachypodium cultivation and plant care.

647

648 **Figure legend**

649 Fig. 1: Tissue differentiation and development of Brachypodium grain. **A**. Brachypodium grain cross-
650 sections from 8 DAF to 41 days after flowering (DAF). Bright-field micrographs of toluidine blue-
651 stained sections. **B**. Fluorescent micrographs of acridine orange-stained sections highlighting the
652 different tissues of the outer layers. **C**. Lipophilic Sudan red staining of Brachypodium grain tissues
653 showing the reactive cuticles (arrows): a thick cuticle outside the testa (t) and a thinner cuticle
654 outside the nucellar epidermis (ne). pe: pericarp, ep: external pericarp, pa: pericarp parenchyma, ne:
655 nucellus epidermis, tub: tubular cells, t: testa, t1: pigmented cells of the testa, t2: cells of the testa
656 underneath the thick cuticle al: aleurone layer, en: endosperm. Bars represent 50 µm in A and C, and
657 10 µm in B.

658 Fig. 2: HPAEC analysis of oligosaccharides produced by Endoxylanase fingerprinting of Brachypodium
659 grain's cell walls. **A**. Oligosaccharides released by digestion with Endoxylanase from Brachypodium
660 whole grains at 8, 20, 28 and 38 DAF. **B**. Oligosaccharides released by digestion with Endoxylanase
661 from dissected endosperm (EN) and outer layers (OL) of Brachypodium grain harvested at 28 and 38
662 DAF.

663 Fig. 3: Arabinoxylan epitopes in Brachypodium developing grain. **A**. Immunofluorescence images
664 localizing arabinoxylan epitopes in the outer layers, the aleurone and the endosperm from 8 to 41
665 DAF of the Brachypodium grain. **B**. TEM of Brachypodium grain at 19 and 41 DAF showing the
666 distribution of immunogold labeling with AX1 and FerAra in the aleurone and in the endosperm. The
667 sections were all treated with Lichenase prior to immunolabeling. Differential interference contrast
668 (DIC) showing the tissue structures and the region where the immunofluorescence acquisitions were
669 taken (black and white squares). Bars represent 20 µm for A and 1 µm for B.

670 Fig. 4: Distribution of cell wall polysaccharides during Brachypodium grain development**.**
671 Immunofluorescent labeling of developing grain (from 8 to 41 DAF) with anti-(1–3) (1–4)-β-D-glucans
672 antibody (MLG), CBM3a, LM21 and LM25. The sections were all treated with Lichenase and Xylanase
673 prior to immunolabeling. Bars represent 20 µm.

674 Fig. 5: Distribution of rhamnogalacturonan I during Brachypodium grain development**.**
675 Immunofluorescent labeling images of developing grain (from 8 to 41 DAF) localizing

676 rhamnogalacturonan I backbone epitope using RUI antibody or galactan and arabinan side chains
677 epitopes using LM5 and LM6 antibodies respectively. The sections were all treated with Lichenase
678 and Xylanase prior to immunolabeling. Framed in orange at the right bottom, a higher magnification
679 highlighting the localization of arabinan near the plasma membrane. Bars represent 20 µm.

680 Fig. 6: Homogalacturonan deposition in developing Brachypodium grain. Immunofluorescence and
681 TEM images localizing methylesterified HG epitope using LM20 (A) and low (or no) methylesterified
682 HG epitope using LM19 antibody (B). The sections were all treated with Lichenase and Xylanase prior
683 to immunolabeling. c: cuticle, cw: cell wall, scw: sub-cell wall layer, b: vesicular bodies, t1: pigmented
684 cells of the testa, t2: cells of the testa underneath the thick cuticle, tub: tubular cells. Bars represent
685 20 µm for fluorescence immunolabeling images, and 1µm for TEM images.

686 Fig. 7: Distribution of polysaccharides into the two layers of the testa. **A.** TEM images showing the
687 distribution of arabinoxylans (AX1 and FerAra antibodies) and xyloglucans (LM25) epitopes in the
688 testa of Brachypodium grain at 19 DAF stages. **B.** TEM images showing the distribution of low
689 methylesterified homogalacturonan, feruloylated arabinoxylans and xyloglucans epitopes in the testa
690 of Brachypodium mature grain (41 DAF) using LM19, anti-FerAra and LM25 antibodies respectively.
691 tub: tubular cells, t1: pigmented cells of the testa, t2: cells of the testa underneath the thick cuticle,
692 c: cuticle. Bars represent 1 µm.

693 Fig. 8: Schematic representation of the immunolabeled detection of polysaccharides in the different
694 tissues of the Brachypodium grain during the development, from the end of the cellularization stage
695 to the maturation of grain. The results are separated in two parts: on the one hand the distribution
696 of polysaccharides into the albumen and aleurone; on the other hand the distribution of
697 polysaccharides into the main structures of the outer layers (pericarp, nucellar epidermis, testa and
698 cuticles). The appreciative abundance of polysaccharides (for a given immunolabeling) is indicated by
699 a thick, a thin or a dotted line.

700

701 **Supplementary data**

702 Fig. S1 : Detection of autofluorescence in Brachypodium developing grains, in the absence of
703 antibodies and at three acquisition times framing those used in this work.

704

705 **References**

706

707 [1] J. Draper, L.A. Mur, G. Jenkins, G.C. Ghosh-Biswas, P. Bablak, R. Hasterok, A.P.
708 Routledge, Brachypodium distachyon. A new model system for functional genomics in
709 grasses, Plant Physiol. 127 (2001) 1539–1555. doi:10.1104/pp.010196.
710 [2] E.A. Kellogg, Brachypodium distachyon as a Genetic Model System., Annu. Rev. Genet.
711 49 (2015) 1–20. doi:10.1146/annurev-genet-112414-055135.
712 [3] D.L. O'Connor, S. Elton, F. Ticchiarelli, M.M. Hsia, J.P. Vogel, T. Leyser, Cross-species
713 functional diversity within the PIN auxin efflux protein family, Elife. 6 (2017).
714 doi:10.7554/eLife.31804.
715 [4] T. International, B. Initiative, Genome sequencing and analysis of the model grass
716 Brachypodium distachyon., Nature. 463 (2010) 763–8. doi:10.1038/nature08747.
717 [5] D.M. Rancour, J.M. Marita, R.D. Hatfield, Cell wall composition throughout
718 development for the model grass Brachypodium distachyon., Front. Plant Sci. 3 (2012)

719 266. doi:10.3389/fpls.2012.00266.
720 [6] U. Christensen, A. Alonso-Simon, H. V. Scheller, W.G.T. Willats, J. Harholt,
721 Characterization of the primary cell walls of seedlings of Brachypodium distachyon - A
722 potential model plant for temperate grasses, Phytochemistry. 71 (2010) 62–69.
723 doi:10.1016/j.phytochem.2009.09.019.
724 [7] A. Betekhtin, A. Milewska-Hendel, J. Lusinska, L. Chajec, E. Kurczynska, R. Hasterok,
725 Organ and tissue-specific localisation of selected cell wall epitopes in the zygotic
726 embryo of Brachypodium distachyon, Int. J. Mol. Sci. 19 (2018).
727 doi:10.3390/ijms19030725.
728 [8] M. Opanowicz, P. Hands, D. Betts, M.L. Parker, G.A. Toole, E.N.C. Mills, J.H. Doonan, S.
729 Drea, Endosperm development in Brachypodium distachyon, J. Exp. Bot. 62 (2011)
730 735–748. doi:10.1093/jxb/erq309.
731 [9] P. Hands, S. Drea, A comparative view of grain development in Brachypodium
732 distachyon, J. Cereal Sci. 56 (2012) 2–8. doi:10.1016/j.jcs.2011.12.010.
733 [10] F. Guillon, B. Bouchet, F. Jamme, P. Robert, B. Quéméner, C. Barron, C. Larré, P.
734 Dumas, L. Saulnier, Brachypodium distachyon grain: Characterization of endosperm
735 cell walls, J. Exp. Bot. 62 (2011) 1001–1015. doi:10.1093/jxb/erq332.
736 [11] F. Guillon, C. Larré, F. Petipas, A. Berger, J. Moussawi, H. Rogniaux, A. Santoni, L.
737 Saulnier, F. Jamme, M. Miquel, L. Lepiniec, B. Dubreucq, A comprehensive overview of
738 grain development in Brachypodium distachyon variety Bd21, J. Exp. Bot. 63 (2012)
739 739–755. doi:10.1093/jxb/err298.
740 [12] E.A. Kellogg, Evolutionary History of the Grasses, Plant Physiol. 125 (2001) 1198–1205.
741 doi:10.1104/pp.125.3.1198.
742 [13] H.L. Wang, J.W. Patrick, C.E. Offler, X.D. Wang, The cellular pathway of photosynthate
743 transfer in the developing wheat grain. III. A structural analysis and physiological
744 studies of the pathway from the endosperm cavity to the starchy endosperm, Plant.
745 Cell Environ. 18 (1995) 389–407. doi:10.1111/j.1365-3040.1995.tb00374.x.
746 [14] S. Krishnan, P. Dayanandan, Structural and histochemical studies on grain-filling in the
747 caryopsis of rice (Oryza sativa L.), J. Biosci. 28 (2003) 455–469.
748 doi:10.1007/BF02705120.
749 [15] R. Palmer, V. Cornuault, S.E. Marcus, J.P. Knox, P.R. Shewry, P. Tosi, Comparative in
750 situ analyses of cell wall matrix polysaccharide dynamics in developing rice and wheat
751 grain, Planta. 241 (2015) 669–685. doi:10.1007/s00425-014-2201-4.
752 [16] R.A. Burton, G.B. Fincher, Current challenges in cell wall biology in the cereals and
753 grasses, Front. Plant Sci. 3 (2012). doi:10.3389/fpls.2012.00130.
754 [17] M. Francin-Allami, K. Merah, C. Albenne, H. Rogniaux, M. Pavlovic, V. Lollier, R. Sibout,
755 F. Guillon, E. Jamet, C. Larré, Cell wall proteomic of Brachypodium distachyon grains:
756 A focus on cell wall remodeling proteins, Proteomics. 15 (2015) 2296–2306.
757 doi:10.1002/pmic.201400485.
758 [18] M. Francin-allami, V. Lollier, M. Pavlovic, H.S. Clemente, H. Rogniaux, E. Jamet, F.
759 Guillon, C. Larré, Understanding the Remodelling of Cell Walls during Brachypodium
760 distachyon Grain Development through a Sub-Cellular Quantitative Proteomic
761 Approach, Proteomes. (2016) 1–16. doi:10.3390/proteomes4030021.
762 [19] M.C. Ralet, O. Tranquet, D. Poulain, A. Moïse, F. Guillon, Monoclonal antibodies to
763 rhamnogalacturonan I backbone, Planta. 231 (2010) 1373–1383. doi:10.1007/s00425-
764 010-1116-y.
765 [20] F. Guillon, O. Tranquet, L. Quillien, J.P. Utille, J.J. Ordaz Ortiz, L. Saulnier, Generation

766 of polyclonal and monoclonal antibodies against arabinoxylans and their use for
767 immunocytochemical location of arabinoxylans in cell walls of endosperm of wheat, J.
768 Cereal Sci. 40 (2004) 167–182. doi:10.1016/j.jcs.2004.06.004.
769 [21] S. Philippe, O. Tranquet, J.P. Utille, L. Saulnier, F. Guillon, Investigation of ferulate
770 deposition in endosperm cell walls of mature and developing wheat grains by using a
771 polyclonal antibody, Planta. 225 (2007) 1287–1299. doi:10.1007/s00425-006-0422-x.
772 [22] P.J. Meikle, N.J. Hoogenraad, I. Bonig, A.E. Clarke, B.A. Stone, A (1-3,1-4)-beta-glucan-
773 specific monoclonal antibody and its use in the quantitation and immunocytochemical
774 location of (1-3,1-4)-beta-glucans, Plant J. 5 (1994) 1–9.
775 [23] Y. Verhertbruggen, S.E. Marcus, A. Haeger, J.J. Ordaz-Ortiz, J.P. Knox, An extended set
776 of monoclonal antibodies to pectic homogalacturonan, Carbohydr. Res. 344 (2009)
777 1858–1862. doi:10.1016/j.carres.2008.11.010.
778 [24] S.E. Marcus, A.W. Blake, T.A.S. Benians, K.J.D. Lee, C. Poyser, L. Donaldson, O. Leroux,
779 A. Rogowski, H.L. Petersen, A. Boraston, H.J. Gilbert, W.G.T. Willats, J.P. Knox,
780 Restricted access of proteins to mannan polysaccharides in intact plant cell walls,
781 Plant J. 64 (2010) 191–203. doi:10.1111/j.1365-313X.2010.04319.x.
782 [25] H.L. Pedersen, J.U. Fangel, B. McCleary, C. Ruzanski, M.G. Rydahl, M.C. Ralet, V.
783 Farkas, L. Von Schantz, S.E. Marcus, M.C.F. Andersen, R. Field, M. Ohlin, J.P. Knox,
784 M.H. Clausen, W.G.T. Willats, Versatile high resolution oligosaccharide microarrays for
785 plant glycobiology and cell wall research, J. Biol. Chem. 287 (2012) 39429–39438.
786 doi:10.1074/jbc.M112.396598.
787 [26] L. Jones, G.B. Seymour, J.P. Knox, Localization of pectic galactan in tomato cell walls
788 using a monoclonal antibody specific to (1-4)-β-D-Galactan., Plant Physiol. 113 (1997)
789 1405–1412. doi:113/4/1405 [pii].
790 [27] W.G.T. Willats, S.E. Marcus, J.P. Knox, Generation of a monoclonal antibody specific to
791 (1→5)-α-l-arabinan, Carbohydr. Res. 308 (1998) 149–152. doi:10.1016/S0008-
792 6215(98)00070-6.
793 [28] A.W. Blake, L. McCartney, J.E. Flint, D.N. Bolam, A.B. Boraston, H.J. Gilbert, J.P. Knox,
794 Understanding the biological rationale for the diversity of cellulose-directed
795 carbohydrate-binding modules in prokaryotic enzymes, J. Biol. Chem. 281 (2006)
796 29321–29329. doi:10.1074/jbc.M605903200.
797 [29] A.L. Chateigner-Boutin, B. Bouchet, C. Alvarado, B. Bakan, F. Guillon, The wheat grain
798 contains pectic domains exhibiting specific spatial and development-associated
799 distribution, PLoS One. 9 (2014). doi:10.1371/journal.pone.0089620.
800 [30] R. Fauré, C.M. Courtin, J.A. Delcour, C. Dumon, C.B. Faulds, G.B. Fincher, S. Fort, S.C.
801 Fry, S. Halila, M.A. Kabel, L. Pouvreau, B. Quemener, A. Rivet, L. Saulnier, H.A. Schols,
802 H. Driguez, M.J. O'Donohue, A brief and informationally rich naming system for
803 Oligosaccharide motifs of heteroxylans found in plant cell walls, Aust. J. Chem. 62
804 (2009) 533–537. doi:10.1071/CH08458.
805 [31] J.J. Ordaz-Ortiz, M.F. Devaux, L. Saulnier, Classification of wheat varieties based on
806 structural features of arabinoxylans as revealed by endoxylanase treatment of flour
807 and grain, J. Agric. Food Chem. 53 (2005) 8349–8356. doi:10.1021/jf050755v.
808 [32] L. Saulnier, P. Robert, M. Grintchenko, F. Jamme, B. Bouchet, F. Guillon, Wheat
809 endosperm cell walls: Spatial heterogeneity of polysaccharide structure and
810 composition using micro-scale enzymatic fingerprinting and FT-IR microspectroscopy,
811 J. Cereal Sci. 50 (2009) 312–317. doi:10.1016/j.jcs.2009.05.003.
812 [33] G. Dervilly, L. Saulnier, P. Roger, J.F. Thibault, Isolation of homogeneous fractions from

813 wheat water-soluble arabinoxylans. Influence of the structure on their
814 macromolecular characteristics, J. Agric. Food Chem. 48 (2000) 270–278.
815 doi:10.1021/jf990222k.
816 [34] B. V. McCleary, T.S. Gibson, D.C. Mugford, Measurement of Total Starch in Cereal
817 Products by Amyloglucosidase-α-Amylase Method: Collaborative Study, J. AOAC Int.
818 80 (1997) 571–579.
819 [35] S. Levigne, M. Thomas, M.C. Ralet, B. Quemener, J.F. Thibault, Determination of the
820 degrees of methylation and acetylation of pectins using a C18 column and internal
821 standards, Food Hydrocoll. 16 (2002) 547–550. doi:10.1016/S0268-005X(02)00015-2.
822 [36] P.L. Freeman, G.H. Palmer, The structure of the pericarp and testa of barley, J. Inst.
823 Brew. 90 (1984) 88–94. doi:10.1002/j.2050-0416.1984.tb04244.x.
824 [37] I.N. Morrison, Ultrastructure of the cuticular membranes of the developing wheat
825 grain, Can. J. Bot. 53 (1975) 2077–2087. doi:10.1139/b75-232.
826 [38] J. De Giorgi, U. Piskurewicz, S. Loubery, A. Utz-Pugin, C. Bailly, L. Mène-Saffrané, L.
827 Lopez-Molina, An Endosperm-Associated Cuticle Is Required for Arabidopsis Seed
828 Viability, Dormancy and Early Control of Germination, PLoS Genet. 11 (2015).
829 doi:10.1371/journal.pgen.1005708.
830 [39] S. Loubéry, J. De Giorgi, A. Utz-Pugin, L. Demonsais, L. Lopez-Molina, A Maternally
831 Deposited Endosperm Cuticle Contributes to the Physiological Defects of *transparent*
832 *testa* Seeds, Plant Physiol. 177 (2018) 1218–1233. doi:10.1104/pp.18.00416.
833 [40] K. Trafford, P. Haleux, M. Henderson, M. Parker, N.J. Shirley, M.R. Tucker, G.B.
834 Fincher, R.A. Burton, Grain development in Brachypodium and other grasses: Possible
835 interactions between cell expansion, starch deposition, and cell-wall synthesis, J. Exp.
836 Bot. 64 (2013) 5033–5047. doi:10.1093/jxb/ert292.
837 [41] J. Beaugrand, D. Crônier, P. Thiebeau, L. Schreiber, P. Debeire, B. Chabbert, Structure,
838 chemical composition, and xylanase degradation of external layers isolated from
839 developing wheat grain, J. Agric. Food Chem. 52 (2004) 7108–7117.
840 doi:10.1021/jf049529w.
841 [42] Y. Yin, D. Mohnen, I. Gelineo -Albersheim, Y. Xu, M.G. Hahn, Glycosyltransferases of
842 the GT 8 Family, Annu. Plant Rev. 41 (2011) 167–212.
843 doi:10.1002/9781444391015.ch6.
844 [43] C. Barron, A. Surget, X. Rouau, Relative amounts of tissues in mature wheat (Triticum
845 aestivum L.) grain and their carbohydrate and phenolic acid composition, J. Cereal Sci.
846 45 (2007) 88–96. doi:10.1016/j.jcs.2006.07.004.
847 [44] Rost F.W.D., Autofluorescence in plants, fungi and bacteria, Fluoresc. Microsc.
848 Cambridge Univ. Press. Vol II (1995) 16–39.
849 [45] W. Baschong, R. Suetterlin, R. Hubert Laeng, Control of autofluorescence of archival
850 formaldehyde-fixed, paraffin-embedded tissue in confocal laser scanning microscopy
851 (CLSM), J. Histochem. Cytochem. 49 (2001) 1565–1571.
852 doi:10.1177/002215540104901210.
853 [46] S. Ho-Yue-Kuang, C. Alvarado, S. Antelme, B. Bouchet, L. Cézard, P. Le Bris, F. Legée, A.
854 Maia-Grondard, A. Yoshinaga, L. Saulnier, F. Guillon, R. Sibout, C. Lapierre, A.L.
855 Chateigner-Boutin, Mutation in Brachypodium caffeic acid O-methyltransferase 6
856 alters stem and grain lignins and improves straw saccharification without
857 deteriorating grain quality, J. Exp. Bot. 67 (2016) 227–237. doi:10.1093/jxb/erv446.
858 [47] S.M. Wilson, R.A. Burton, M.S. Doblin, B.A. Stone, E.J. Newbigin, G.B. Fincher, A. Bacic,
859 Temporal and spatial appearance of wall polysaccharides during cellularization of

860 barley (Hordeum vulgare) endosperm, Planta. 224 (2006) 655–667.
861 doi:10.1007/s00425-006-0244-x.
862 [48] P. Robert, F. Jamme, C. Barron, B. Bouchet, L. Saulnier, P. Dumas, F. Guillon, Change in
863 wall composition of transfer and aleurone cells during wheat grain development,
864 Planta. 233 (2011) 393–406. doi:10.1007/s00425-010-1306-7.
865 [49] S. Philippe, L. Saulnier, F. Guillon, Arabinoxylan and (1 → 3),(1 → 4)-β-glucan
866 deposition in cell walls during wheat endosperm development, Planta. 224 (2006)
867 449–461. doi:10.1007/s00425-005-0209-5.
868 [50] M.C. Hernandez-Gomez, M.G. Rydahl, A. Rogowski, C. Morland, A. Cartmell, L. Crouch,
869 A. Labourel, C.M.G.A. Fontes, W.G.T. Willats, H.J. Gilbert, J.P. Knox, Recognition of
870 xyloglucan by the crystalline cellulose-binding site of a family 3a carbohydrate-binding
871 module, FEBS Lett. 589 (2015) 2297–2303. doi:10.1016/j.febslet.2015.07.009.
872 [51] Y. Zheng, X. Wang, Y. Chen, E. Wagner, D.J. Cosgrove, Xyloglucan in the primary cell
873 wall: assessment by FESEM, selective enzyme digestions and nanogold affinity tags,
874 Plant J. 93 (2018) 211–226. doi:10.1111/tpj.13778.
875 [52] G. Gartaula, S. Dhital, G. Netzel, B.M. Flanagan, G.E. Yakubov, C.T. Beahan, H.M.
876 Collins, R.A. Burton, A. Bacic, M.J. Gidley, Quantitative structural organisation model
877 for wheat endosperm cell walls: Cellulose as an important constituent, Carbohydr.
878 Polym. 196 (2018) 199–208. doi:10.1016/j.carbpol.2018.05.041.
879 [53] V.G. de la Calle, C.B. Sicilia, P.C. Zalduegui, R.I. Fernandez, Mannans and endo-beta-
880 mannanases (MAN) in Brachypodium distachyon: expression profiling and possible
881 role of the BdMAN genes during coleorhiza-limited seed germination, J. Exp. Bot. 66
882 (2015) 3753–3764. http://oa.upm.es/40461/.
883 [54] L. Saulnier, F. Guillon, A.L. Chateigner-Boutin, Cell wall deposition and metabolism in
884 wheat grain, J. Cereal Sci. 56 (2012) 91–108. doi:10.1016/j.jcs.2012.02.010.
885 [55] T.K. Pellny, A. Lovegrove, J. Freeman, P. Tosi, C.G. Love, J.P. Knox, P.R. Shewry, R.A.C.
886 Mitchell, Cell Walls of Developing Wheat Starchy Endosperm: Comparison of
887 Composition and RNA-Seq Transcriptome, Plant Physiol. 158 (2012) 612–627.
888 doi:10.1104/pp.111.189191.
889 [56] S.M. Wilson, R.A. Burton, H.M. Collins, M.S. Doblin, F.A. Pettolino, N. Shirley, G.B.
890 Fincher, A. Bacic, Pattern of Deposition of Cell Wall Polysaccharides and Transcript
891 Abundance of Related Cell Wall Synthesis Genes during Differentiation in Barley
892 Endosperm, Plant Physiol. 159 (2012) 655–670. doi:10.1104/pp.111.192682.
893 [57] L. Tyler, J.N. Bragg, J. Wu, X. Yang, G.A. Tuskan, J.P. Vogel, Annotation and
894 comparative analysis of the glycoside hydrolase genes in Brachypodium distachyon,
895 BMC Genomics. 11 (2010). doi:10.1186/1471-2164-11-600.
896 [58] M. Strohmeier, M. Hrmova, M. Fischer, A.J. Harvey, G.B. Fincher, J. Pleiss, Molecular
897 modeling of family GH16 glycoside hydrolases: potential roles for xyloglucan
898 transglucosylases/hydrolases in cell wall modification in the poaceae., Protein Sci. 13
899 (2004) 3200–3213. doi:10.1110/ps.04828404.
900 [59] M. Hrmova, V. Farkas, J. Lahnstein, G.B. Fincher, A barley xyloglucan xyloglucosyl
901 transferase covalently links xyloglucan, cellulosic substrates, and (1,3;1,4)-β-D-
902 glucans, J. Biol. Chem. 282 (2007) 12951–12962. doi:10.1074/jbc.M611487200.
903 [60] W.G.T. Willats, L. Mccartney, W. Mackie, J.P. Knox, Pectin: Cell biology and prospects
904 for functional analysis, Plant Mol. Biol. 47 (2001) 9–27.
905 doi:10.1023/A:1010662911148.
906 [61] K.H. Caffall, D. Mohnen, The structure, function, and biosynthesis of plant cell wall

907 pectic polysaccharides, Carbohydr. Res. 344 (2009) 1879–1900.
908 doi:10.1016/j.carres.2009.05.021.
909 [62] S. Wolf, G. Mouille, J. Pelloux, Homogalacturonan methyl-esterification and plant
910 development, Mol. Plant. 2 (2009) 851–860. doi:10.1093/mp/ssp066.
911 [63] J.-Y. Gou, L.M. Miller, G. Hou, X.-H. Yu, X.-Y. Chen, C.-J. Liu, Acetylesterase-Mediated
912 Deacetylation of Pectin Impairs Cell Elongation, Pollen Germination, and Plant
913 Reproduction, Plant Cell. 24 (2012) 50–65. doi:10.1105/tpc.111.092411.
914 [64] G.B. Fincher, Revolutionary Times in Our Understanding of Cell Wall Biosynthesis and
915 Remodeling in the Grasses, Plant Physiol. 149 (2009) 27–37.
916 doi:10.1104/pp.108.130096.
917 [65] K. Niedojadło, M. Hyjek, E. Bednarska-Kozakiewicz, Spatial and temporal localization
918 of homogalacturonans in Hyacinthus orientalis L. ovule cells before and after
919 fertilization, Plant Cell Rep. 34 (2015) 97–109. doi:10.1007/s00299-014-1690-8.
920 [66] M.A. Atmodjo, Z. Hao, D. Mohnen, Evolving Views of Pectin Biosynthesis, Annu. Rev.
921 Plant Biol. 64 (2013) 747–779. doi:10.1146/annurev-arplant-042811-105534.
922 [67] F. Sénéchal, C. Wattier, C. Rustérucci, J. Pelloux, Homogalacturonan-modifying
923 enzymes: Structure, expression, and roles in plants, J. Exp. Bot. 65 (2014) 5125–5160.
924 doi:10.1093/jxb/eru272.
925 [68] G. López-Casado, A.J. Matas, E. Domínguez, J. Cuartero, A. Heredia, Biomechanics of
926 isolated tomato (Solanum lycopersicum L.) fruit cuticles: The role of the cutin matrix
927 and polysaccharides, J. Exp. Bot. 58 (2007) 3875–3883. doi:10.1093/jxb/erm233.
928
929

Figure 1

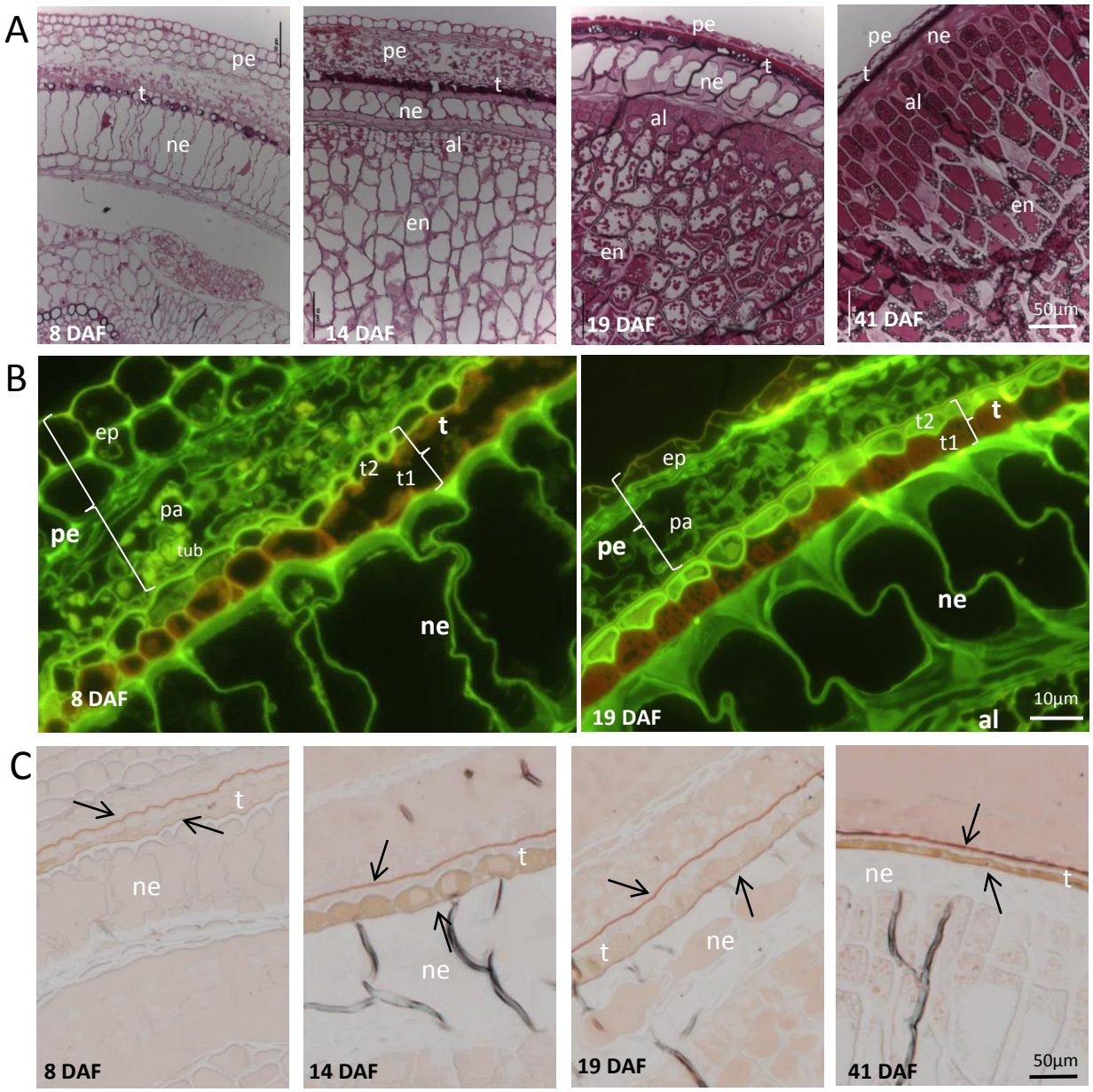
A
pe
t
ne
8 DAF
pe
t
ne
al
en
14 DAF
pe
t
ne
al
en
19 DAF
pe
ne
t
al
en
41 DAF
50µm
B
ep
pe
pa
tub
t
t2
t1
ne
8 DAF
ep
pe
pa
t2
t1
t
ne
19 DAF
10µm
al
C
t
ne
8 DAF
t
ne
14 DAF
t
ne
19 DAF
ne
t
41 DAF
50µm

Figure 2

A

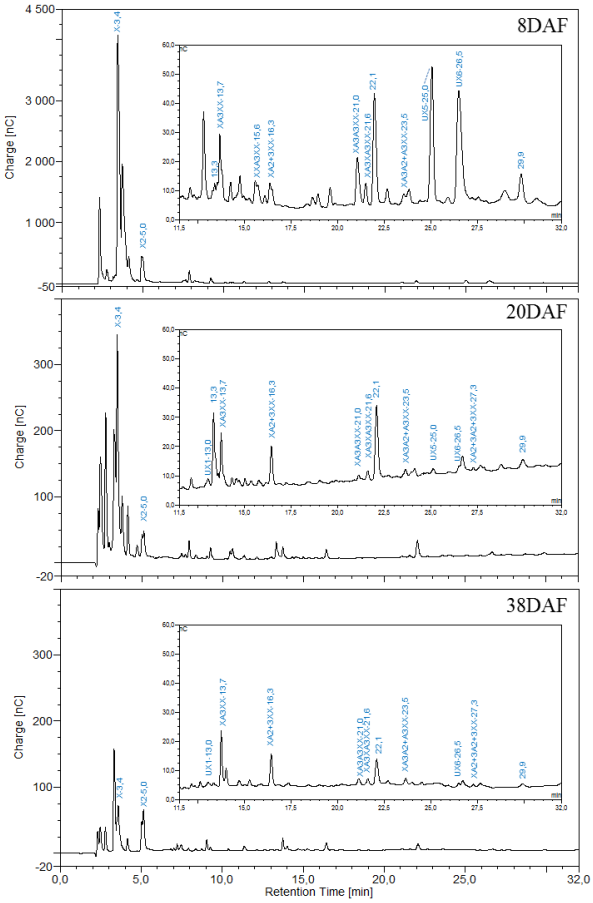
8DAF
20DAF
38DAF
Charge [nC]
Retention Time [min]

B

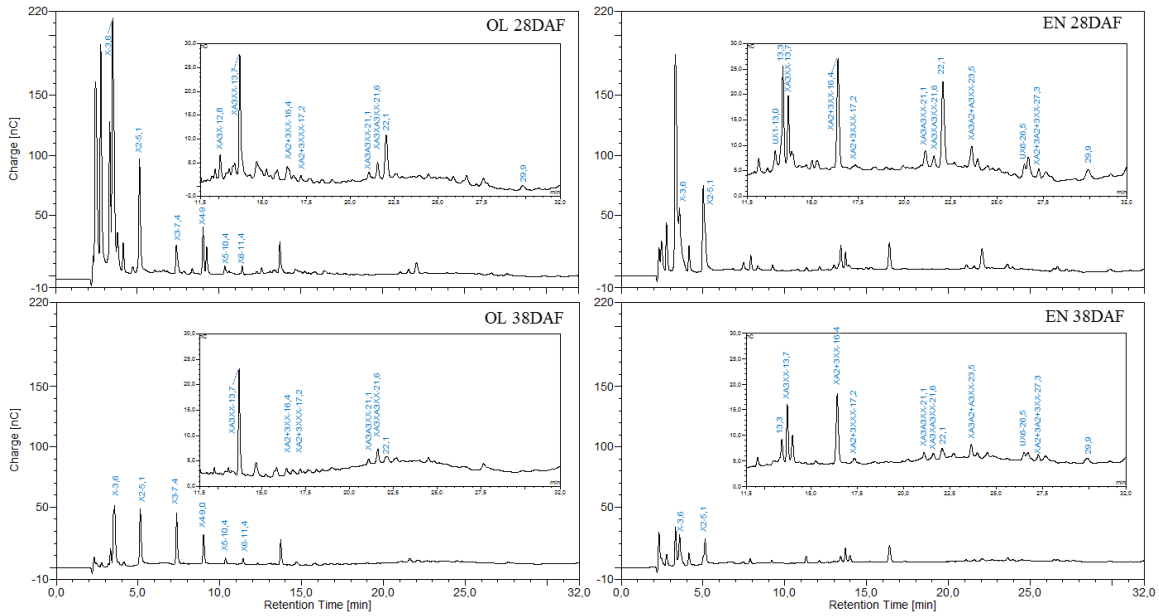
OL 28DAF
EN 28DAF
OL 38DAF
EN 38DAF
Charge [nC]
Retention Time [min]

Figure 3

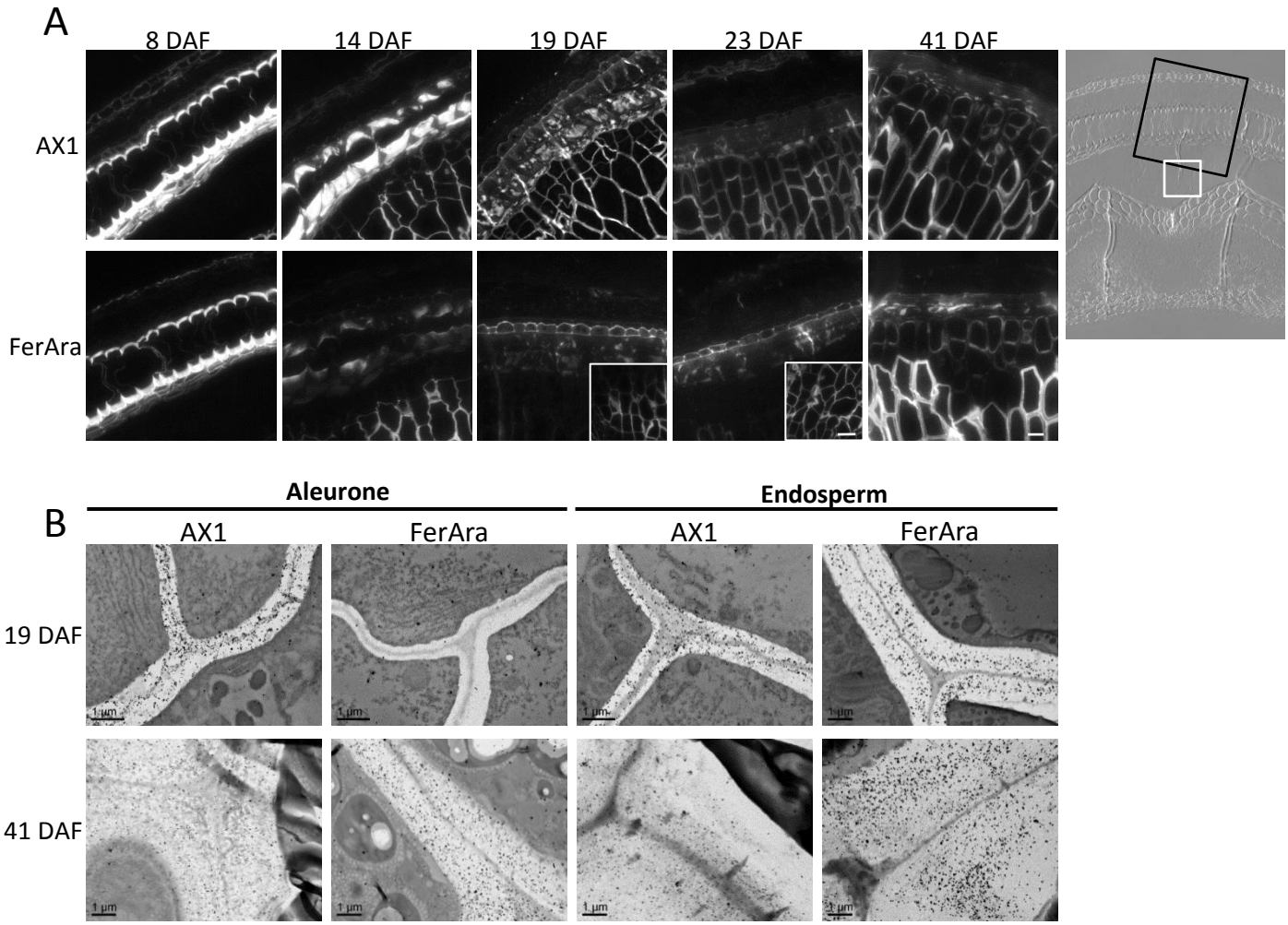
A
8 DAF
14 DAF
19 DAF
23 DAF
41 DAF
AX1
FerAra
B
Aleurone
Endosperm
AX1
FerAra
AX1
FerAra
19 DAF
41 DAF
1 µm

Figure 4

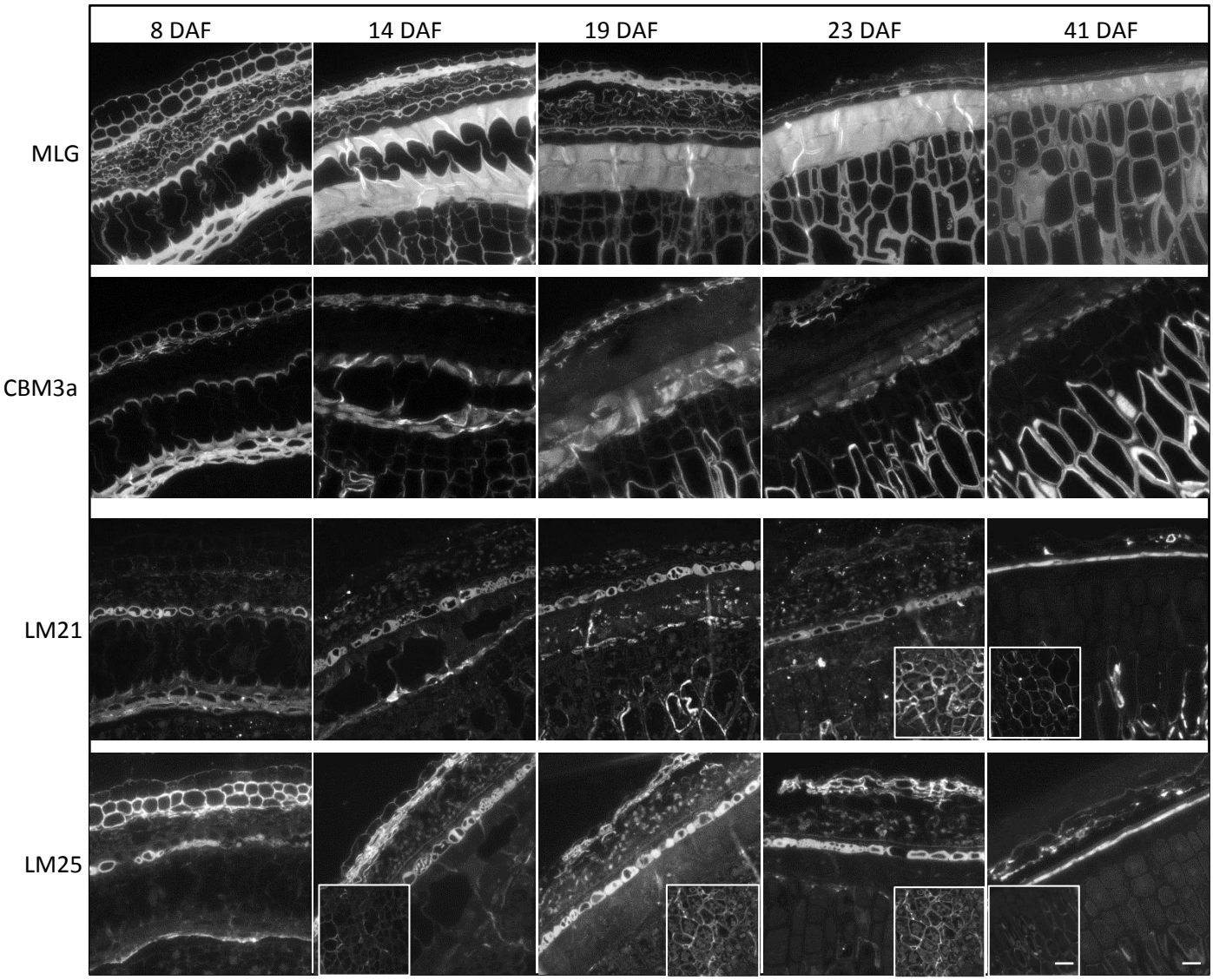

Figure 5

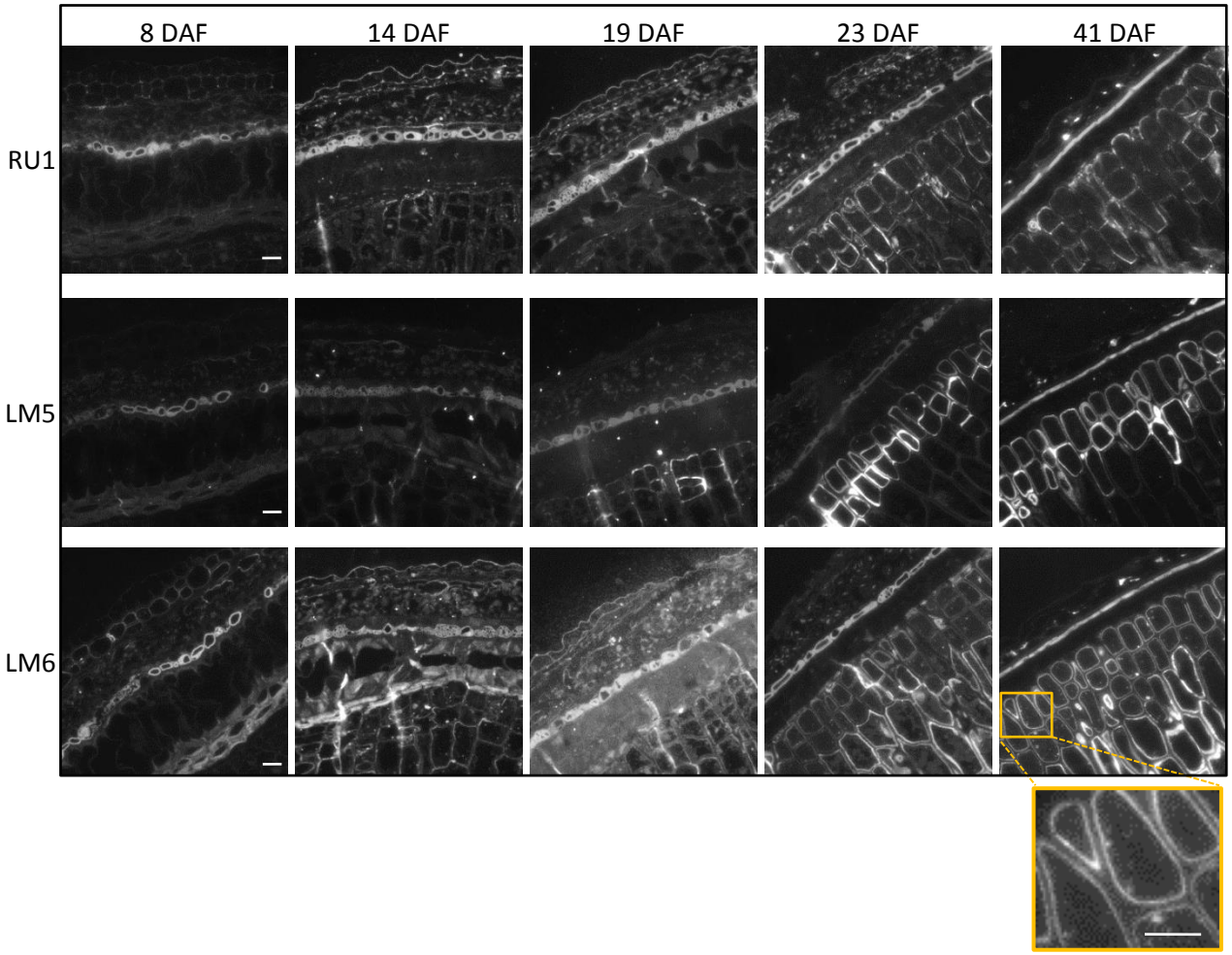

Figure 6

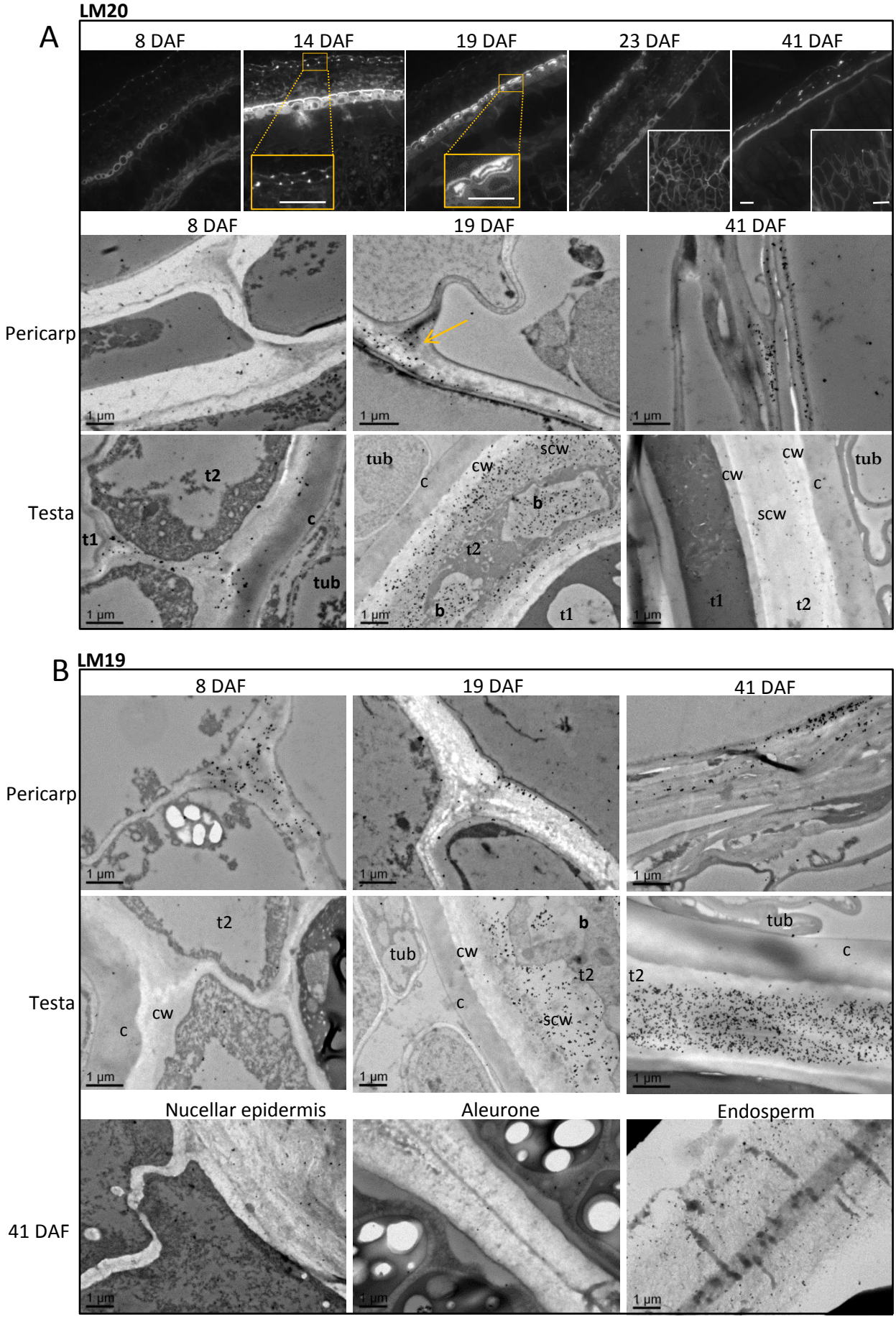
A
LM20
8 DAF
14 DAF
19 DAF
23 DAF
41 DAF
8 DAF
19 DAF
41 DAF
Pericarp
Testa
1 µm
t2
c
t1
tub
cw
scw
b
B
LM19
Nucellar epidermis
Aleurone
Endosperm
41 DAF

Figure 7

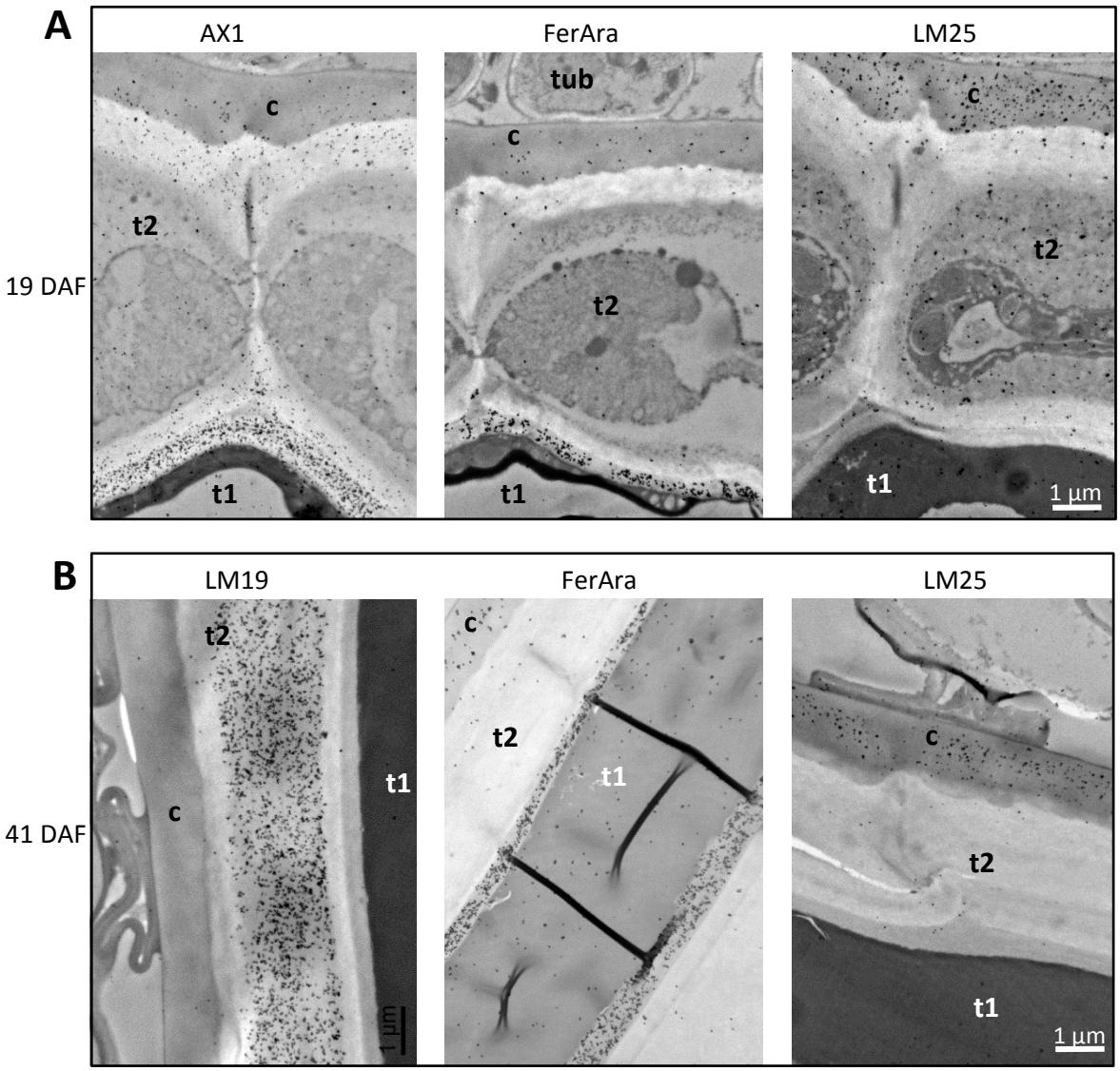
A
AX1
FerAra
LM25
19 DAF
c
t2
t1
tub
c
t2
t1
c
t2
t1
1 µm
B
LM19
FerAra
LM25
41 DAF
t2
c
t1
1 µm
c
t2
t1
c
t2
t1
1 µm

Figure 8

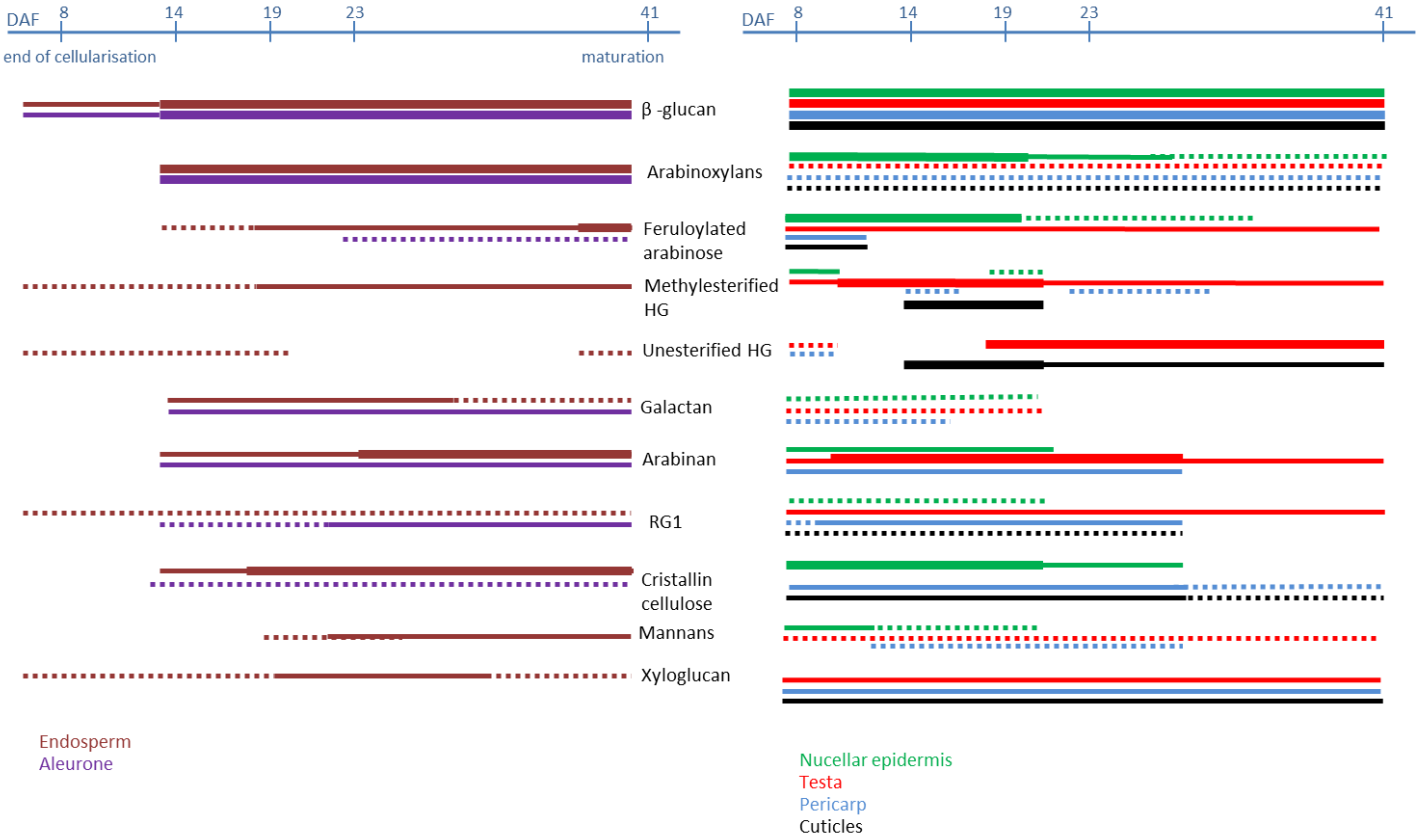
DAF
8
14
19
23
41
end of cellularisation
maturation
β -glucan
Arabinoxylans
Feruloylated arabinose
Methylesterified HG
Unesterified HG
Galactan
Arabinan
RG1
Cristallin cellulose
Mannans
Xyloglucan
Endosperm
Aleurone
Nucellar epidermis
Testa
Pericarp
Cuticles